

LITHOGEOCHEMICAL AND Nd ISOTOPIC DATA FOR HUNT RIVER BELT AND WEEKES AMPHIBOLITE, HOPEDALE BLOCK, LABRADOR: EVIDENCE FOR TWO STAGES OF MAFIC MAGMATISM AT >3200 AND ~3100 Ma

H.A.I. Sandeman, A.M. Hinchey¹, D. Diekrup¹ and H.E. Campbell²

Mineral Deposits Section

¹Regional Geology Section

²Terrain Sciences and Geoscience Data Management Section

ABSTRACT

Widespread Mesoarchean Maggo orthogneiss and late Mesoarchean granitoid rocks of the Kanairiktok Intrusive Suite occur in the Hopedale Block, southern Nain Craton, Labrador. These units host common, metre- to kilometre-scale rafts, xenoliths and boudins of fine- to medium-grained hornblende ± garnet amphibolite, massive coarse-grained peridotite varying to harzburgite (Weekes Amphibolite) and locally, less common iron-rich sedimentary rocks and psammites. These rafts occur marginal (northwest and southeast) to the Mesoarchean (ca. 3100 Ma) Hunt River Belt, an elongate (~75-km-long) and narrow (<5-km-wide), northeast-trending supracrustal belt consisting mostly of fine-grained amphibolite, minor iron formation, and sparse felsic volcanic and semipelitic to arenitic rocks. Primary volcanic textures in all amphibolites are lacking, contact relationships of the Hunt River Belt with the engulfing granitoids are absent and basement to the Hunt River Belt and basal unconformities have not been identified. Thus, the relationships between the Hunt River Belt, the Weekes Amphibolite and the Maggo Gneiss are unclear. This contribution examines lithogeochemical and Nd isotopic data for amphibolites of the Hunt River Belt and isolated rafts of Weekes Amphibolite and ultramafic rocks, to address their origin, and to constrain their relationships with the Maggo Gneiss and Kanairiktok Intrusive Suite. The data suggest that the rocks referred to as the Weekes Amphibolite may reflect two distinct temporal origins, one contemporaneous with the Maggo Gneiss formation (>3200 Ma) the other with the younger Hunt River Belt (~3100 Ma).

INTRODUCTION AND REGIONAL SETTING

The Hopedale Block of Labrador forms the southern structural domain of the Nain Craton, which together with the northern Saglek Block (Bridgewater and Schiøtte, 1991), form the western part of the North Atlantic Craton (Bridgewater *et al.*, 1973), a wedge-shaped Archean domain bounded on three sides by Paleoproterozoic orogens (Figure 1). The Hopedale Block lacks crust older than ca. 3300 Ma and has a tectonometamorphic history, prior to ca. 2800 Ma, distinct from that of the Saglek Block. Most of the Hopedale Block consists of a variably deformed granitoid basement complex termed the Maggo Gneiss (Figure 2; Ermanovics and Raudsepp, 1979; Finn, 1989a, b, 1991; Ermanovics, 1993; James, 1997; James *et al.*, 1996, 2002). The Maggo Gneiss was intruded by the Archean, mafic Hopedale dykes sometime after the poorly defined >3100 Ma Hopedalian tectonothermal event (Korstgård and Ermanovics, 1985; James *et al.*, 2002). These dykes have never been dated, and

lithogeochemistry is lacking. Two supracrustal (greenstone) belts are recognized: the Hunt River Belt, a ca. 3105 Ma, elongate (~75-km-long) and narrow (<5-km-wide) north-northeast-trending amphibolite-facies supracrustal belt in the centre of the block and; the ca. 3000 Ma, ~65-km-long and <6-km-wide greenschist- to amphibolite-facies grade north-northeast-trending Florence Lake Belt in the southeast (Figure 2). The Hopedale Block also contains numerous smaller mafic belts preserved as narrow lens and rafts surrounded by orthogneiss and granitoid intrusions. Although sometimes referred to as the Weekes association supracrustal rocks (*e.g.*, Schiøtte *et al.*, 1989; Finn, 1991), herein these are collectively termed the Weekes Amphibolite.

The Maggo Gneiss, Weekes Amphibolite and supracrustal rocks of the Hunt River and Florence Lake belts were collectively deformed and metamorphosed during the ca. 2960–2880 Ma, greenschist- to amphibolite-facies Fiordian tectonometamorphic event, associated with the for-

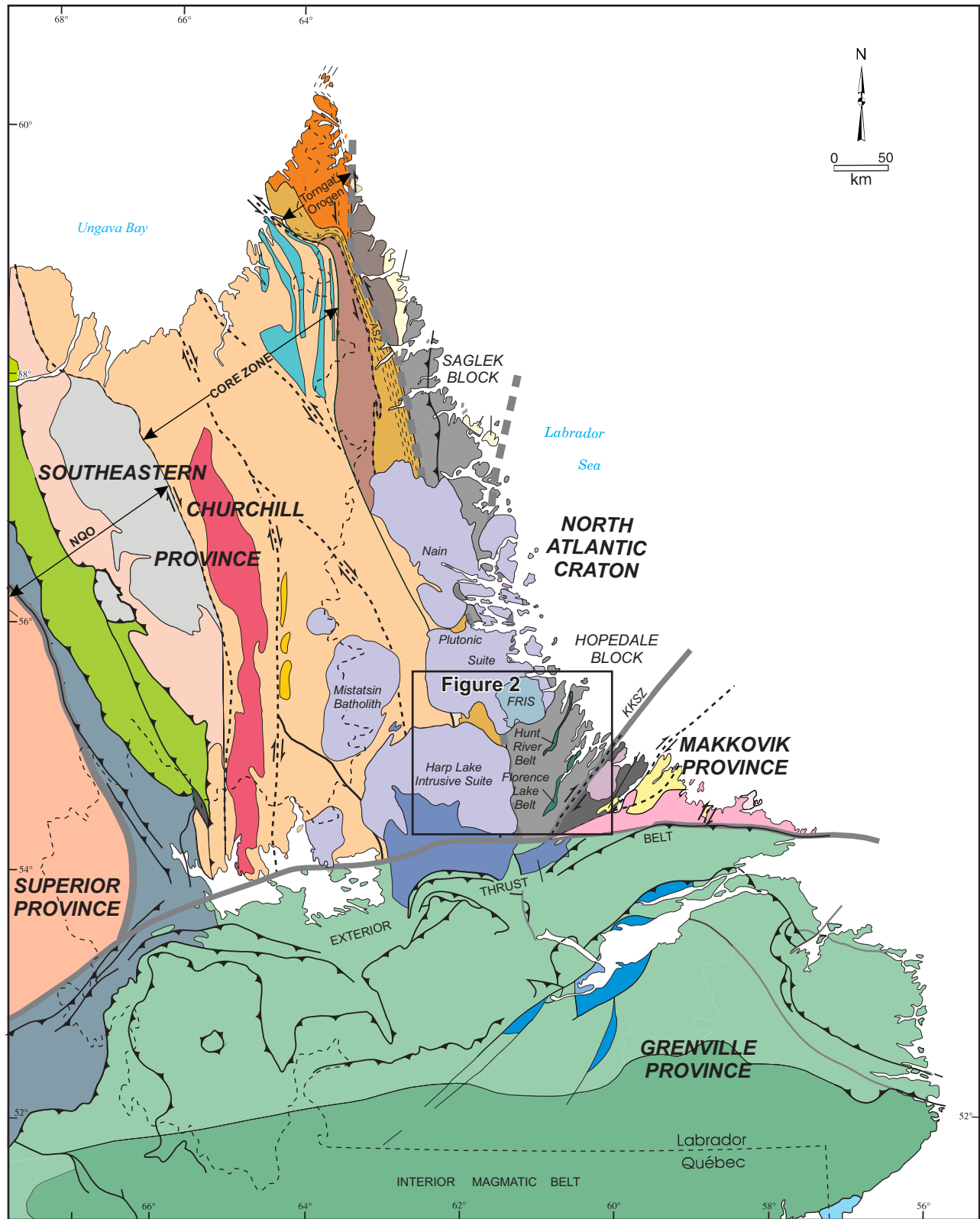
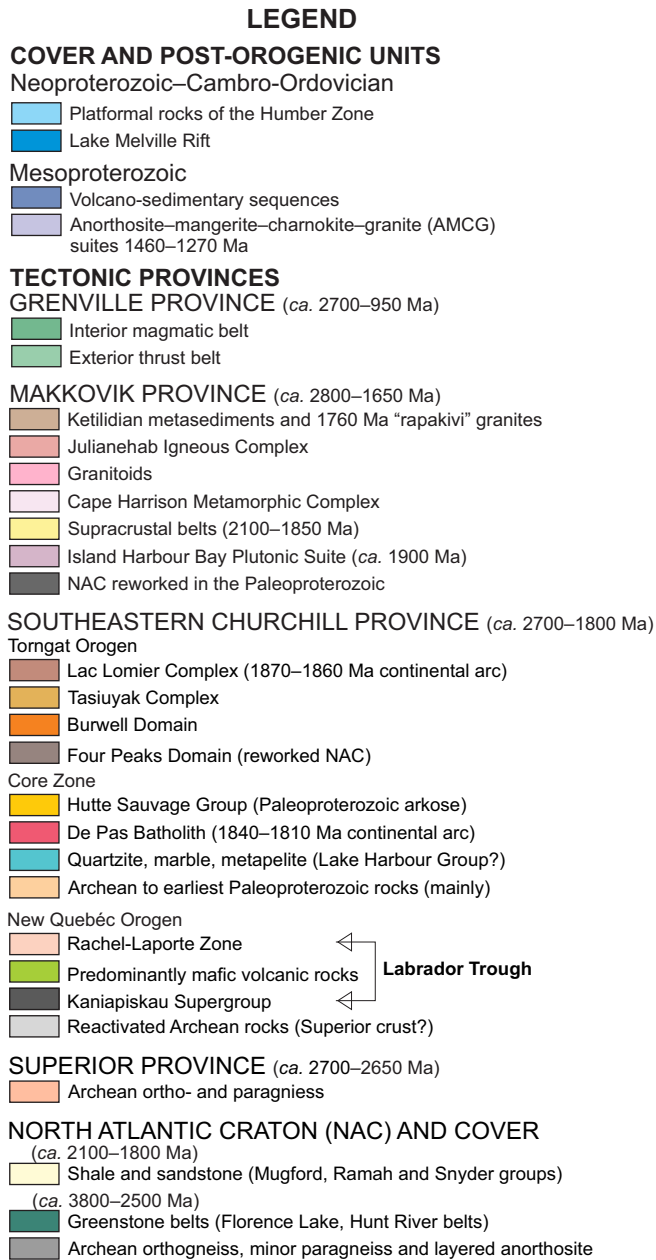


Figure 1. Simplified geological map of the northeastern Canadian Shield of Labrador and Québec showing the location of the Hopedale map sheet with respect to major geological terranes. Modified from Hinchey et al. (2023). KKSZ=Kanairiktok Shear Zone; FRIS=Flowers River Igneous Suite; NGO=New Québec Orogen; ASZ=Ablviak Shear Zone.



SYMBOLS

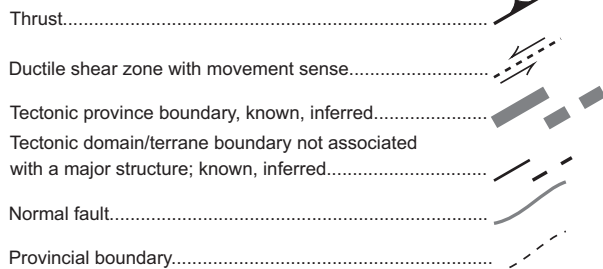


Figure 1. Legend.

mation of penetrative, northeast-striking structures. All rocks are intruded by variably deformed tonalitic to granitic and granite pegmatite intrusive rocks of the ca. 2890 and 2825 Ma Kanairiktok Intrusive Suite (Ermanovics and Raudsepp, 1979; Ermanovics *et al.*, 1982; Loveridge *et al.*, 1987; Ermanovics, 1993; Wasteneys *et al.*, 1996; James *et al.*, 2002; Rayner, 2022). These engulf and surround the older units and were intruded in the latter stages, and locally postdate, the Fiordian event (Ermanovics *et al.*, 1982; Korstgård and Ermanovics, 1985; Ermanovics, 1993; James *et al.*, 2002).

In the western parts of the Hopedale Block (Figure 2), the Paleo- to Mesoarchean, upper amphibolite- to granulite-facies Maggo Gneiss and Weekes Amphibolite were intruded by a series of relatively small, 2-km-thick or less, sills, sheets and plugs of late Neoarchean (ca. 2570 Ma) syenite, monzodiorite, essexite (alkali gabbro) and minor syenogranite of the Aucoin Suite (Sandeman and Rafuse, 2011; Sandeman and McNicoll, 2015; Rayner, 2022).

The Archean rocks of the Hopedale Block are intruded by suites of Proterozoic mafic dykes including, from oldest to youngest: the Mesoarchean (?) Hopedale dykes (Korstgård and Ermanovics 1985); the north-northeast to north-south-trending 2238 to 2216 Ma Kikkertavak Suite (Cadman *et al.*, 1993; Sahin and Hamilton, 2019); a single dated north-northeast-trending dyke at 2169 ± 13 Ma (Sahin and Hamilton, *op. cit.*); the northwest-trending ca. 2050 Ma Ellen Island dykes (Sahin and Hamilton, *op. cit.*); a single ca. 1800 Ma northwest-trending (“Ussiranniak Lake”) dyke (Sahin and Hamilton, *op. cit.*); a suite of ca. 1640 Ma, mesotoleucocratic, amphibole ± biotite porphyritic diorite (lamprophyric) sills termed the Kokkorvik sills (Cadman, 1991) and; the northeast-trending, ca. 1273 Ma Harp Dykes (Krogh, 1992, 1993; Cadman *et al.*, 1993). The Kokkorvik sills were proposed, for an unknown reason, to have been emplaced at ca. 1640 Ma (Cadman, 1991), however, based on a thermal ionization mass spectrometry U–Pb abraded titanite age of 1662 ± 4 Ma, and on petrography and limited geochemistry, they may be the same as shallowly dipping, dioritic dykes in the Makkovik Orogen to the south (Sparkes *et al.*, 2010).

In the west, the boundary between the southeast Churchill and Nain provinces and the Torngat orogen is stitched by the anorthosite–mangerite–charnockite–granite association (AMCG) rocks of the ca. 1460 Ma Harp Lake intrusion (Emslie, 1980). In the northern parts of the Hopedale Block, the Archean and Paleoproterozoic rocks are cut by the long-lived, ca. 1363–1292 Ma Nain Plutonic Suite (Hill, 1982; Ryan *et al.*, 1991; Thomas and Morrison, 1991; Tettelaar, 2004) and by the ca. 1293–1271 Ma

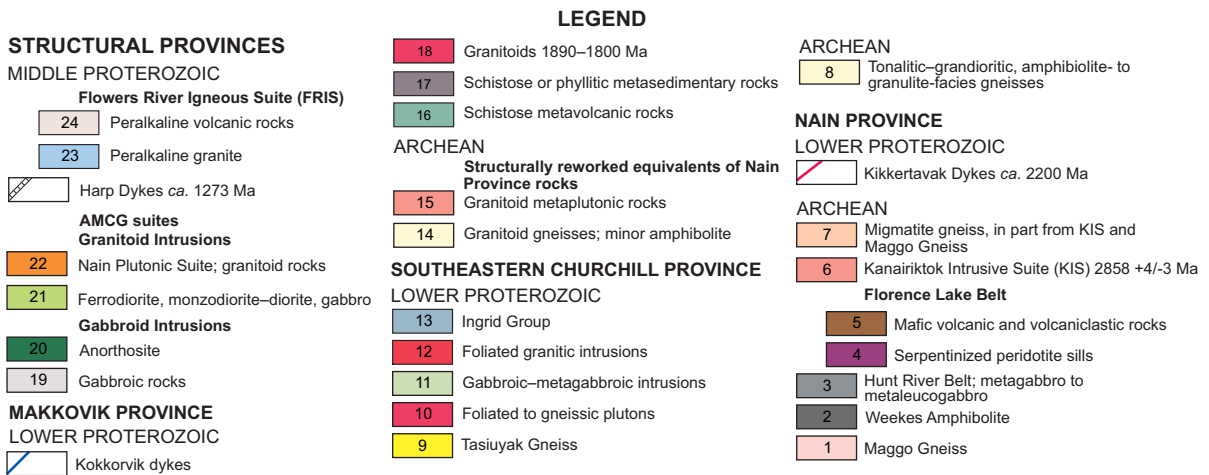
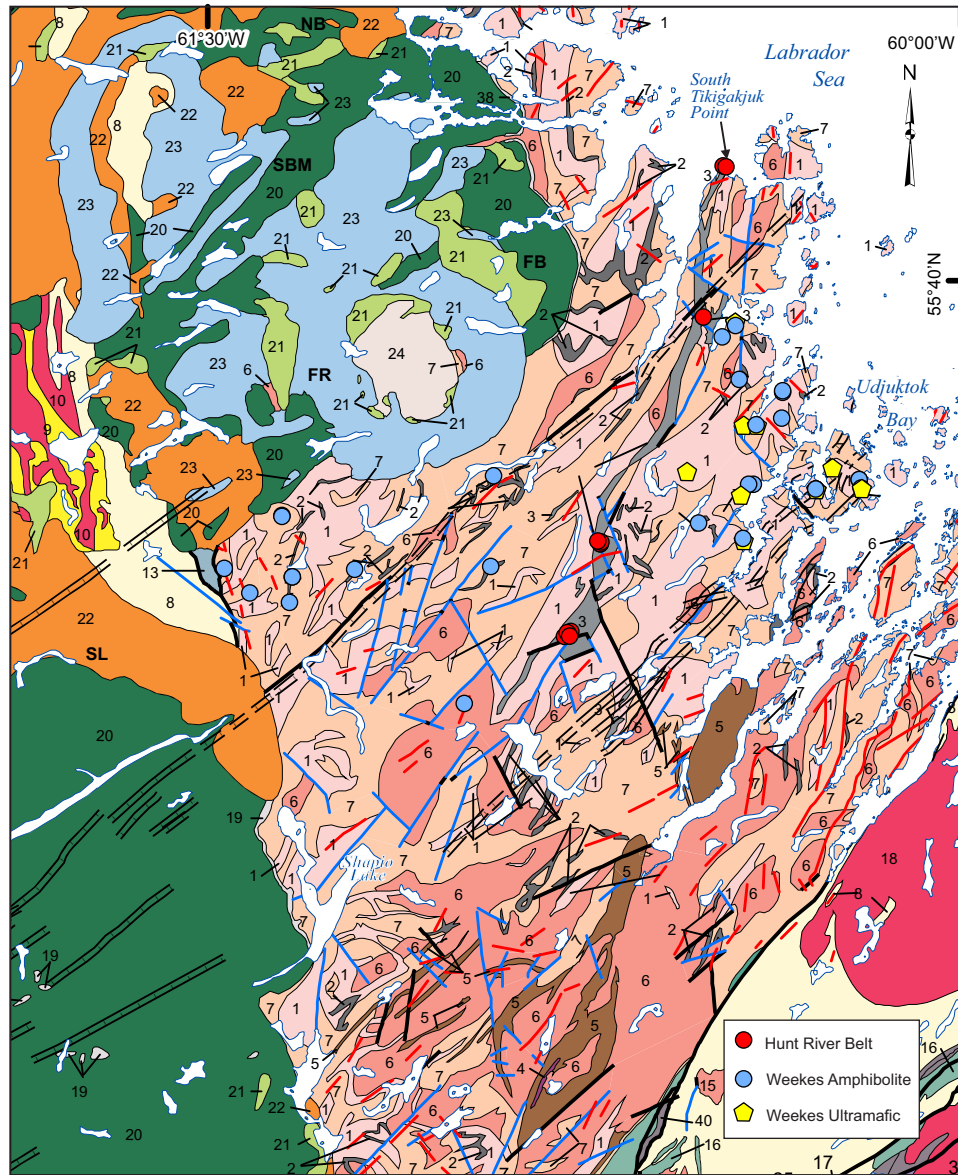


Figure 2. Geology of the Hopedale map area (modified from Hinchey et al., 2023) showing the location of localities discussed in the text and the locations of the samples under investigation.

Flowers River Intrusive Complex (Hill, 1982; Brooks, 1982, 1983; Krogh, 1993; Thomas and Morrison, 1991; Ducharme *et al.*, 2021). The major Archean geological components of the Hopedale Block, possible unconformities and tectono-thermal events are depicted in Figure 3.

THE HUNT RIVER BELT

The Hunt River Belt stretches from the Labrador Sea coast at South Tikigakjuk Point, southwestward for approximately 75 km to north of Shapio Lake (Figure 2) and is divided into northern, central and southern segments (James *et al.*, 2002). The central and southern parts of the belt preserve the thickest and most complete stratigraphy. The compositionally layered supracrustal rocks define a number of

kilometric-scale antiforms with south-southwest-trending axial planes and moderately plunging fold axes (Ermanovics, 1993; James *et al.*, 2002). The supracrustal belt is dominated by mafic metavolcanic rocks with greatly subordinate felsic volcanic, ultramafic and contemporaneous metasedimentary rocks (*see* James *et al.*, 2002). The amphibolite-facies metavolcanic and metasedimentary rocks are encompassed by the Maggo orthogneiss and all were intruded by granitoid rocks of the Kanairiktok Plutonic Suite. The Hunt River Belt has been studied by Taylor (1972, 1977, 1979), Jesseau (1976), Ermanovics and Raudsepp (1982, 1993), James (1997) and James *et al.* (2002). These studies provide further observational background for the foundation of our discussion.

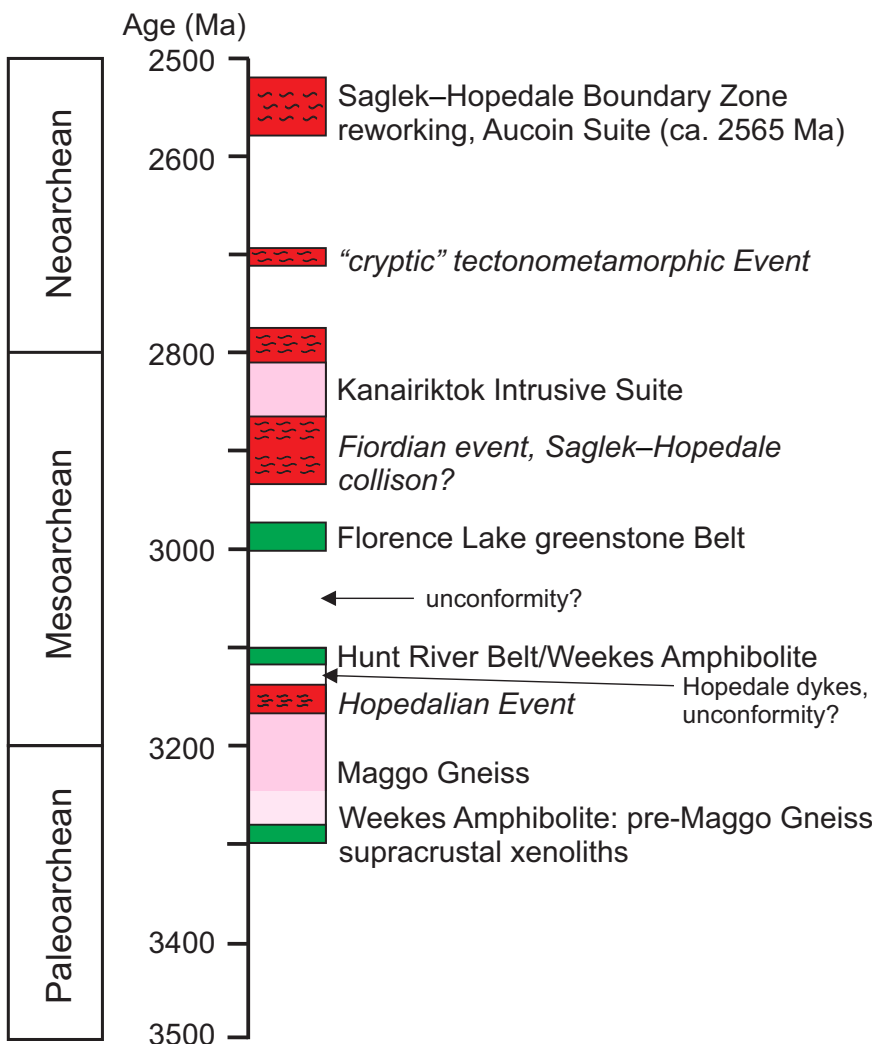


Figure 3. Lithotectonic stratigraphic architecture and known and inferred ages of geological units and tectonometamorphic and erosional events of the Hopedale map sheet. Modified after James *et al.* (2002) with data from Sandeman and McNicoll (2015), Ducharme *et al.* (2021) and Rayner (2022).

Sites visited herein consisted of interlayered sequences of typically 10s to 100 metre-scale fine-grained amphibolite with ~30–50-cm-scale layered feldspar- and hornblende-rich layers as well as local pyrite–pyrrhotite-rich horizons (Plate 1A). The latter may represent iron-rich exhalative deposits. Locally, amphibolite consists of wispy discontinuous, feldspar-rich layers interlayered with a greater modal percent of amphibole. These may represent metamorphosed bedded mafic tuffs (Plate 1B). Ultramafic rocks are less common than the amphibolites and typically form relatively narrow (<10-m-wide) lenses and layers in amphibolite (Plate 1C). Stratigraphic facing direction indicators are absent.

Representative thin sections, covering many of the widely separated sample localities reveal that most of the Hunt River Belt samples consist of fine-grained, sugary, weakly layered and variably foliated amphibolite, typically consisting of 20–30 volume % plagioclase and 60–80% dark-green hornblende (Plate 1D). Garnet, clinopyroxene and orthopyroxene are less common and typically form granular aggregates in specific compositional layers in the amphibolites. Accessory phases include: actinolite, epidote and chlorite after hornblende, biotite, apatite and magnetite. Pyrite and pyrrhotite are common and may comprise up to 8–10% of some rusty samples.

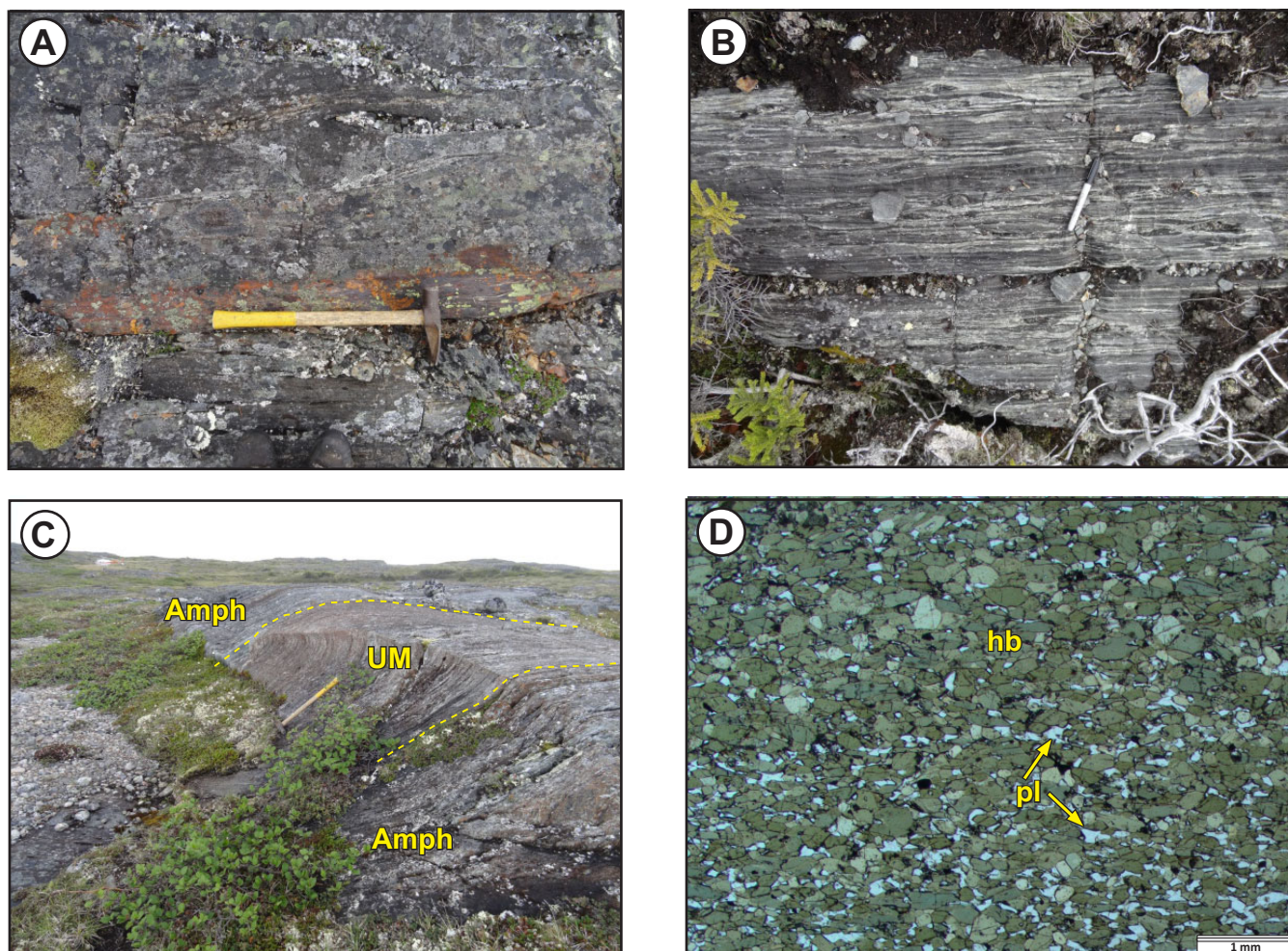


Plate 1. Photographs of representative amphibolite exposed in the Hunt River Belt. A) A 30- to 50-cm-scale-layered amphibolite with a 20-cm-thick pyrrhotite + pyrite-rich layer. Central Hunt River Belt (18HS-007); B) Wispy feldspar-rich layers in a heterogeneous Hunt River amphibolite (near 18HS-007) that may represent a basaltic tuff; C) Well-foliated amphibolite of the Hunt River Belt with an approximately 4-m-thick ultramafic schist horizon (19HS-028); D) Plane-polarized light photomicrograph of granoblastic to weakly nematoblastic amphibolite (18HS-007A) consisting of hornblende, plagioclase and magnetite.

THE WEEKES AMPHIBOLITE

Common rafts and xenoliths of coarser grained, layered amphibolite, ultramafic and sparse metasedimentary rock bodies in Maggo Gneiss were termed the Weekes Amphibolite (Ermanovics and Raudsepp, 1979). These were interpreted as the oldest rocks in the region and were considered to represent dispersed remnants of the previously more widespread Hunt River Belt (Taylor, 1977, 1979; Ermanovics and Raudsepp, 1979; Ermanovics, 1993; James *et al.*, 2002). The possibility was raised, however, that some of these supracrustal rafts and xenoliths may represent pre-Hunt River Belt mafic assemblages formed earlier, or at the same time as the Maggo Gneiss (*see* James *et al.*, 2002). This suggestion is, in part, based on the work of Schiøtte *et al.* (1989) who obtained an age of 3258 ± 24 Ma for what

were interpreted as low-U detrital zircons from a sample of Weekes metasedimentary rock from the Hopedale Block. These data represent the only direct geochronological constraint on the age of the Weekes Amphibolite.

Most amphibolite rafts range from 3 to 6 m thick and 6 to 200 m in length, but larger bodies, hundreds of metres in length locally occur north, west and south of Hopedale. These bodies are typically variably veined by granitoids (*e.g.*, Plate 2A, B) and are associated with hornblendite, ultramafic rocks and sparse metasedimentary rocks. Gneissic tonalite, which may represent Maggo Gneiss and/or gneissic Kanairiktok tonalite, is marginal to and engulfs all Weekes unit rafts. Individual feldspar- and hornblende-dominant layers in the amphibolite typically vary from 2 to 100 cm thick (*e.g.*, Plate 2C) and contain hornblende, pla-

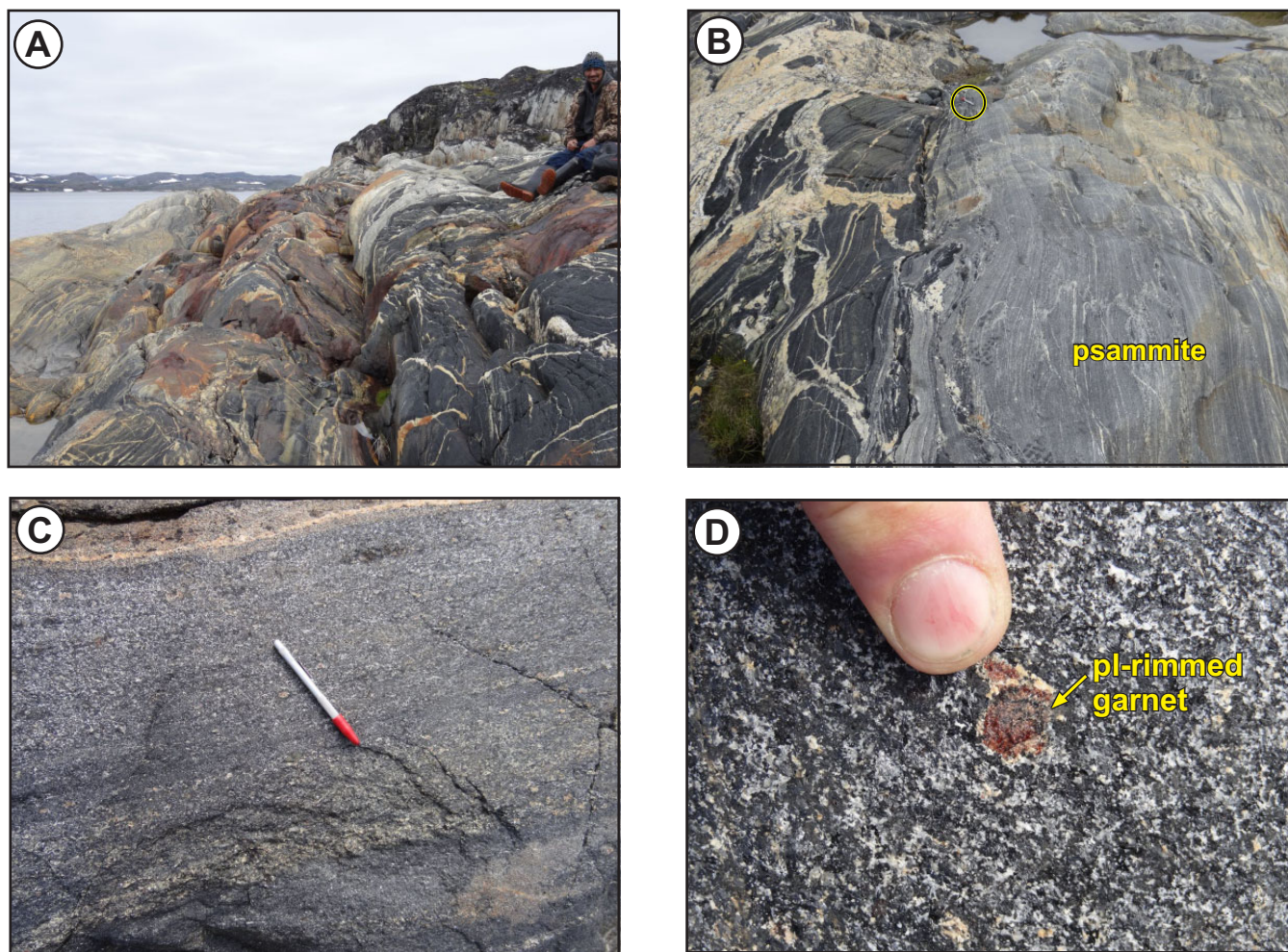


Plate 2. Photographs and photomicrograph of representative rocks of Weekes Amphibolite. A) Granodiorite- and granite pegmatite-veined hornblendite (right) and amphibolite (left) at Tooksooner Bay immediately south of Hopedale airport (Figure 2: 19HS-007). Prospector Edmund Saunders for scale; B) Granite pegmatite-veined hornblendite–amphibolite at left and lighter grey, less-veined psammite at right. Sharpie marker for scale in yellow circle; C) Medium-grained garnetiferous amphibolite at 19HS-007. Note plagioclase rim (P-decrease metamorphic reaction) on garnet; D) Close-up of plagioclase-rimmed garnet in C.

gioclase, garnet (Plate 2D, E), diopside (Plate 2F) and rare biotite and orthopyroxene. Secondary, greenschist-facies grade retrograde metamorphic assemblages include: actinolite/tremolite, grunerite–cummingtonite, epidote, biotite, chlorite and carbonate.

A suite of 22 lithochemical samples of intact and unveined amphibolite, occurring as large-scale, 25 to 100s of metre-scale rafts in the Hopedale map area and spatially separated from the Hunt River Belt, were collected to obtain a better understanding of the origin and tectonic setting of formation of these rocks. The samples are dominantly composed of variably foliated, fine- to medium-grained (1–8 mm) amphibolite to hornblendite (Plate 2E, F), with subordinate garnet amphibolite. Massive garnet amphibolite was noted in numerous localities across the map area and is

locally accompanied by clinopyroxene with and without orthopyroxene. Although no unambiguous primary volcanic textures were noted and most of the exposures of Weekes Amphibolite consist of massive to weakly layered amphibolite, at one locality (19HS-018) elongate (<40 cm), typically oblate and rounded mafic amphibolitic enclaves in a weakly layered, more feldspathic matrix (Plate 2G) were noted. A number of these enclaves have more feldspathic or garnetiferous cores suggesting primary compositional differences between the enclaves and host. Approximate sample locations and their distribution are shown in Figure 2.

Ultramafic examples of Weekes Amphibolite are more common than previously reported and vary from metre-scale ultramafic boudins to hundreds of metre-scale, composite ultramafic and hornblenditic rafts and xenoliths sur-

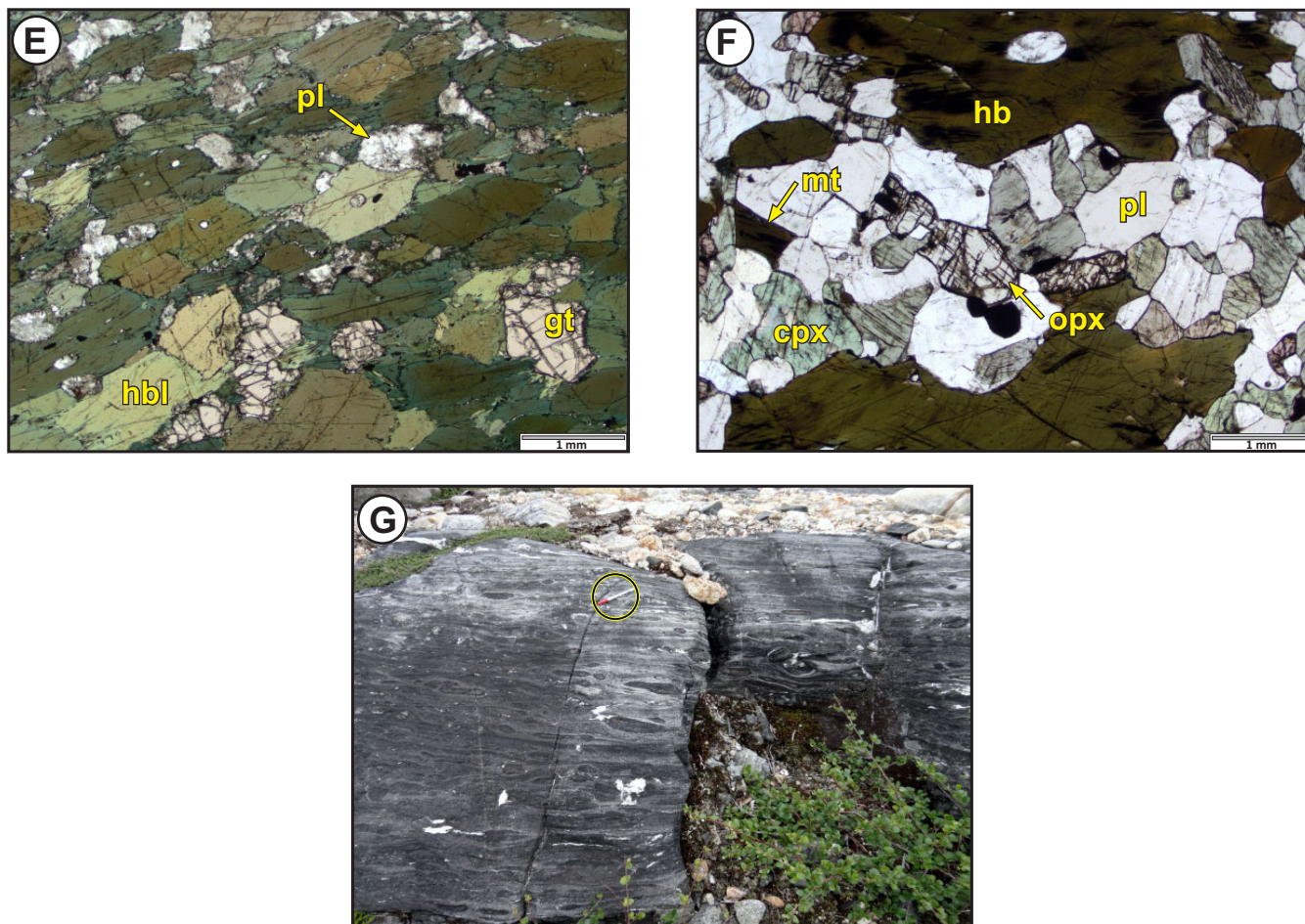


Plate 2 (continued). *E*) Medium- to coarse-grained garnet amphibolite (19HS-007) under plane-polarized light; *F*) Medium- to coarse-grained orthopyroxene-clinopyroxene-bearing amphibolite (19HS017A) under plane-polarized light; *G*) Elongate (<40 cm), typically oblate and rounded mafic amphibolitic enclaves in a weakly layered, more feldspathic matrix (sample 19HS-018). Pen magnet for scale in yellow circle.

rounded by tonalitic gneiss and locally foliated granitoids (e.g., Plate 3A). Rafts and boudins of coarse-grained, serpentinized ultramafic rocks comprising parts of the Weekes Amphibolite unit occur sporadically throughout the block but are apparently more common in areas lying to the east side of the Hunt River Belt and nearer the Labrador Sea coast. These typically consist of massive, medium- to coarse-grained (2–10 mm), variably serpentinized and altered peridotite (Plate 3B), although smaller boudins consist of ultramafic schist. Most of the samples comprise coarse, remnant xenoblastic orthopyroxene surrounded by a serpentinized matrix containing small remnant xenoblastic olivine with rare magnetite and spinel (Plate 3C, D).

FIELD SAMPLING AND ANALYTICAL METHODS

In 2018, under the umbrella of the National Geoscience and Mapping (GEM-II) project, the Geological Survey of

Canada (GSC) completed a 100-m line-spacing airborne aeromagnetic survey over the Hopedale map sheet (NTS 13N; Coyle, 2019). Follow-up in the summers of 2018 and 2019 focused on characterizing the regional rock-types and explaining the distinct magnetic anomalies and patterns of the region via local traversing and helicopter-supported sampling and mapping. During approximately 6 weeks, >100 field stations and 59 samples of the Weekes Amphibolite and ultramafic rocks and, amphibolite of the Hunt River Belt were documented. These were selected using the 1:250 000-scale map of Ermanovics (1993), the new geophysical data (Coyle, *op. cit.*) and the more detailed maps of James *et al.* (2002).

LITHOGEOCHEMICAL METHODS

Clean, representative 1- to 1.5-kg samples were crushed to ~1-cm rock chips and a 50–100 g split was then pulverized in a mild steel pulveriser. All samples were analyzed at

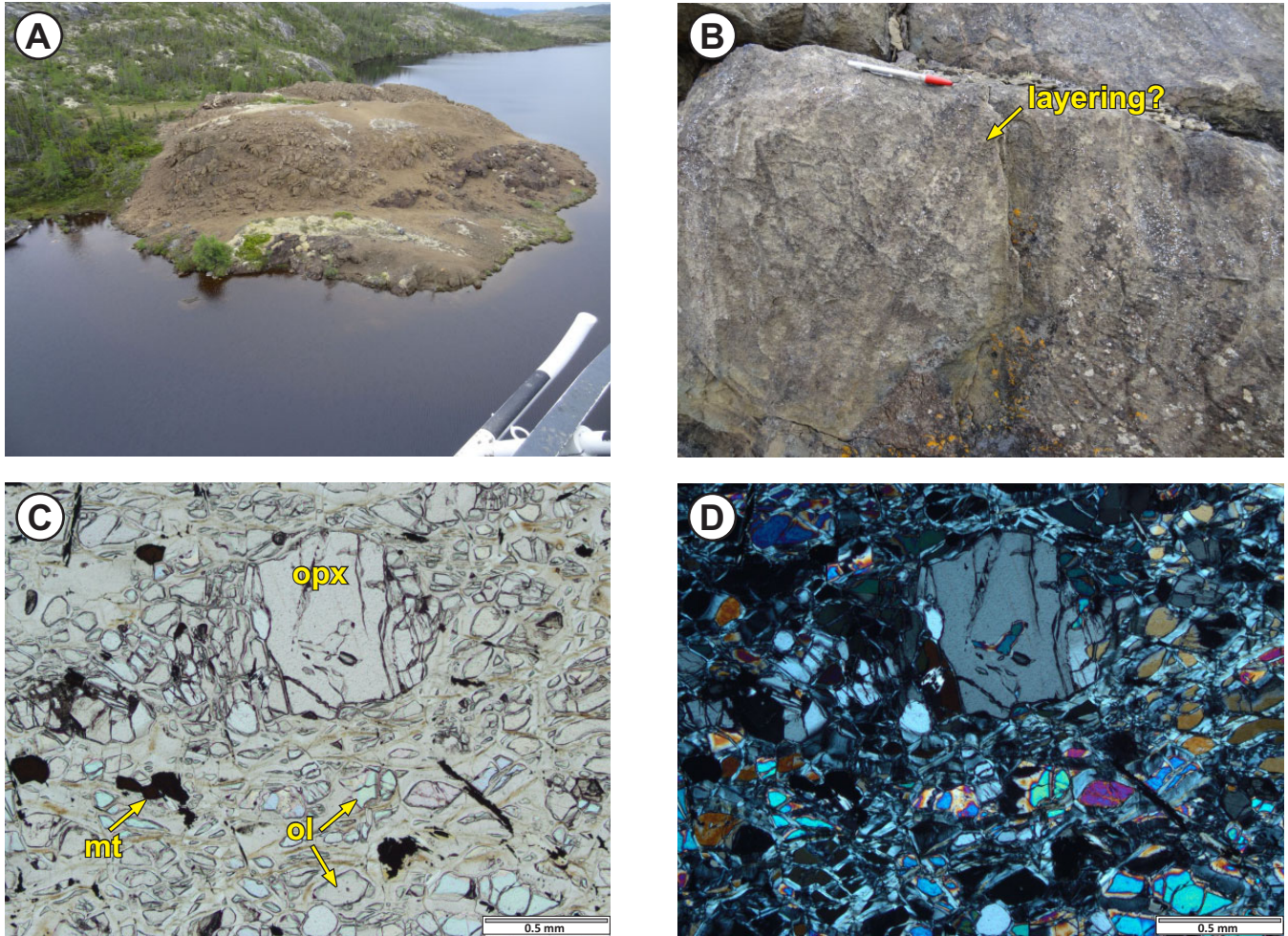


Plate 3. Photographs and photomicrographs of representative rocks of Weekes ultramafic units. A) Oblique aerial photograph looking south at a large (>125-m-long) raft/boudin of coarse-grained peridotite in north–south-trending tonalitic gneiss (locality 19HS-019); B) Outcrop photograph of the bleached, broadly layered, coarse-grained serpentinized orthopyroxene-rich peridotite at locality 19HS-019; C) Photomicrograph in plane-polarized light of coarse-grained, xenoblastic orthopyroxene in a serpentinized groundmass composed of small, relict, xenoblastic olivine and rare magnetite and spinel; D) Same as C but under crossed polars.

the Geochemical laboratory of the Geological Survey of Newfoundland and Labrador (GSNL) following the methods of Finch *et al.* (2018). Major elements were analyzed by ICP-OES after borate fusion. FeO was determined through titration ($\text{Fe}_2\text{O}_3^{\text{T}}$ is the total iron as ferric oxide) and Fe_2O_3 was calculated from the other two iron analyses. Loss on ignition (LOI) was determined through gravimetry. Trace elements were determined using both ICP-MS following borate fusion, and ICP-OES following four-acid digestion. Silver was determined through ICP-OES following nitric acid digestion. An ion selective electrode (ISE) was used to analyze fluoride. A suite of 27 elements, in particular Au, Sb and Se, were analyzed by Instrumental Neutron Activation Analysis (INAA) at Bureau Veritas Laboratories (<https://www.bvlabs.com>). Major elements are reported in wt. % and trace elements are reported in ppm except for Au,

which is given in ppb. Negative detection limit values represent analyses below the detection limit and -99 represents samples that were not analyzed for that element. All litho-geochemical data are in Hinchey *et al.* (2021) but salient litho-geochemical aspects of the Hunt River Belt and Weekes Amphibolite, as well as for the Weekes ultramafic rocks are in Table 1.

Nd ISOTOPE GEOCHEMICAL METHODS

Sm–Nd Analyses Conducted at Memorial University of Newfoundland

Whole-rock powders were weighed into Savilex© Teflon capsules and then spiked with a mixed $^{150}\text{Nd}/^{149}\text{Sm}$ spike before being dissolved using an 8 ml (4:1) mixture of

Table 1. Salient lithochemical features of the Hunt River Belt, Weekes Amphibolite and Weekes ultramafic units

Variable ID	Hunt River Belt			Weekes Amphibolite			Weekes ultramafics			
	max	min	mean	max	min	mean	max	min	mean	
Mg#	68.72	15.15	48.22	71.73	30.20	51.39	96.45	54.87	81.46	
MgO	wt%	12.18	0.97	6.96	9.75	5.08	7.26	44.53	7.39	28.05
TiO ₂	wt%	1.50	0.41	0.83	1.65	0.28	0.93	0.49	0.02	0.20
Al ₂ O ₃	wt%	15.59	8.08	13.18	16.34	6.42	14.22	10.67	0.35	3.85
FeO ^T	wt%	13.58	9.68	11.61	25.66	6.85	12.42	13.51	2.80	9.26
P ₂ O ₅	wt%	0.12	0.03	0.06	0.11	0.03	0.06	0.03	0.00	0.01
Al		49.26	26.34	38.09	49.00	32.41	38.99	99.88	52.19	84.87
CPPI		94.96	76.03	87.17	98.16	80.19	86.44	99.96	89.24	97.63
Cr	ppm	734	34	292	416	45	222	7221	174	2554
Co	ppm	73	12	57	66	35	54	199	64	110
Cu	ppm	1425	66	265	800	8	148	827	3	111
Ni	ppm	254	30	132	159	45	104	3666	69	1421
(La/Yb) _{CN}		3.57	0.11	1.43	6.14	0.16	1.47	9.68	0.57	3.28
(La/Sm) _{CN}		2.02	0.15	1.01	4.14	0.13	1.16	8.72	0.74	2.70
(Gd/Yb) _{CN}		0.25	0.15	0.21	0.31	0.16	0.21	0.83	0.12	0.43
(Th/La) _{CN}		12.84	0.39	2.47	3.50	0.28	0.98	1.70	0.37	1.31
(Th/Nb) _{CN}		5.83	1.06	2.37	6.22	0.64	2.01	2.49	0.85	1.70
(Th/La) _{CN}		12.84	0.39	2.47	3.50	0.28	0.98	1.70	0.30	1.17
Eu/Eu*		2.75	1.85	2.31	2.74	1.82	2.26	3.67	1.12	2.49
Zr/Y		7.68	2.18	4.05	3.89	1.95	2.86	14.00	1.56	4.86
Nb/Y		0.39	0.08	0.19	0.19	0.05	0.09	1.00	0.15	0.49
Nb/Yb		3.70	0.70	1.72	1.67	0.47	0.77	10.00	1.29	5.09

29 M HF – 15 M HNO₃. After five days of acid digestion on a hotplate, the solution was then evaporated to dryness and taken back up in 6M HCl for 4–5 days. The sample was dried down then re-dissolved in 2.5 M HCL. Samples were then loaded into a column containing cation exchange resin AG-50W-X8, H⁺ form, 200–400 mesh where a Sr fraction, if required, can be isolated followed by collection of bulk rare-earth elements (REEs). This bulk solution was then dried and taken up in 0.18 M HCl and loaded on a second column containing Eichrom© Ln resin (50–100 mesh) to isolate Sm and Nd separately from the other REEs. All reagents were purified to ensure a low contamination level.

The Sm and Nd concentrations were determined using a multi-collector Finnigan Mat 262 mass spectrometer (TIMS) set to dynamic mode for isotopic composition determination. Instrumental mass fractionations of Sm and Nd were corrected using a Raleigh law relative to $^{146}\text{Nd}/^{144}\text{Nd} = 0.7219$, $^{152}\text{Sm}/^{147}\text{Sm} = 1.783$. The reported $^{143}\text{Nd}/^{144}\text{Nd}$ ratios were corrected for the deviation from repeated duplicates of the standards JNdi-1 ($^{143}\text{Nd}/^{144}\text{Nd} = 0.512115$; Tanaka *et al.*, 2000). Replicates of the standards yielded a 6-month mean value of $^{143}\text{Nd}/^{144}\text{Nd} = 0.512095 \pm 09$ (1SD, n=27) for JNdi-1. The Nd isotopic results for selected samples are in Table 2.

Sm–Nd Analyses Conducted at Carleton University, Ottawa

Samples were prepared in the clean lab of the Isotope Geochronology and Geochemistry Research Centre (IGGRC) at Carleton University. Rock powders were doped with a ^{148}Nd – ^{149}Sm mixed spike before being dissolved in a mixture of concentrated HF and HNO₃. Sample solution were dried down, and the residues were sequentially dissolved in 7M HNO₃ and in 6M HCl and were final dried down to dryness. The sample residues were dissolved in 1.5 ml of 2.5 M HCl and were loaded onto 14-ml Bio-Rad borosilicate glass chromatography columns containing 3.0 ml of Bio-Rad AG50W-X8 cation exchange resin. Columns were washed with 16 ml of 2.5 M HCl before Sr was eluted in 7 ml 2.5 M HCl. The columns were then washed with 3.5 ml of 6 M HCl before REE were eluted using 9 ml of 6M HCl. The REE fractions were dissolved in 0.26M HCl and were loaded onto 2 ml prepacked Ln resin columns (Eichrom Technologies, LLC, USA). Nd was eluted using 0.26M HCl, followed by Sm elution using 0.5M HCl.

In addition, the Sr fractions were re-cleaned to remove excessive Rb and other impurities using columns containing about 100 microlitres of Sr-Spec resin (Eichrom

Table 2. Nd isotopic data for selected rocks of the Hunt River Belt, Weekes Amphibolite and Weekes ultramafic units

Ref#	SampleID	LabNum	UTMEast	UTMNorth	NTS_map	Lithology	Unit	Nd ppm	Sm ppm	¹⁴⁷ Sm/ ¹⁴⁴ Nd	¹⁴³ Nd/ ¹⁴⁴ Nd	f(Sm/Nd)	Epsilon (ε=3100 Ma)	Init.(t)	Chur(t)	T(DM)D
1	17AH009A01	6540829	638552	6127910	13N/07	metabasalt	HRB	3.85	14.94	0.1555	0.511865	-0.209456024	-15.1	0.508680	0.508609	3158
2	18HS007A	8941472	642850	6139470	13N/07	amphibolite	HRB	5.85	1.88	0.1939	0.512674	-0.0140	0.7	0.508702	0.508609	2996
3	19HS028	8941685	655217	6168112	13N/10	amphibolite	HRB	6.65	2.17	0.197	0.5128	0.001525165	3.2	0.508765	0.508609	2218
4	19HS035A	8941697	657647	6186918	13N/16	hornblende	HRB	3.3	1.18	0.2161	0.513156	0.098627351	10.1	0.508730	0.508609	N/A
5	18AH033A02	6540836	629284	6147819	13N/07	amphibolite	WA	2.90	8.59	0.2042	0.512900	0.038129131	5.1	0.508718	0.508609	2313
6	18HS003A	8941467	674994	6148150	13N/08	garnetiferous amphibolite	WA	6.14	2.07	0.2045	0.512893	0.0394	5.0	0.508705	0.508609	2594
7	18HS033B	8941504	604372	6134682	13N/06	amphibolite	WA	6.04	2.10	0.2099	0.513008	0.0670	7.2	0.508710	0.508609	1280
8	18HS034A	8941506	599157	6132649	13N/06	amphibolite	WA	9.29	2.41	0.1571	0.511964	-0.2013	-13.1	0.508747	0.508609	2961
9	18HS040C	8941518	669541	6146786	13N/08	garnet	WA	7.63	2.55	0.2019	0.512819	0.0266	3.5	0.508683	0.508609	3292
10	19HS038B	8941704	660618	6140263	13N/08	amphibolite	WA	4.99	1.22	0.1475	0.511576	-0.250127097	-20.7	0.508555	0.508609	3475
11	19HS041B	8941521	665143	6155666	13N/09	ultramafic schist	WU	3.77	1.03	0.1658	0.512099	-0.1572	-10.5	0.508704	0.508609	3080
12	19HS009C	8941652	657313	6187019	13N/16	foliated granodiorite	HRB	14.91	1.79	0.0727	0.510199	-0.6304	-47.6	0.508710	0.508609	3109
13	18HS026	8941494	610241	6140743	13N/06	tonalitic gneiss	KIS	26.67	3.95	0.0967	0.510860	-0.5084	-34.7	0.509041	0.508937	2872
14	19HS003A	8941638	626218	6119273	13N/03	foliated monzogranite	KIS	233.73	22.49	0.0581	0.510228	-0.7046	-47.0	0.509135	0.508937	2778
15	18CXAD038B01	N/A	652311	6115497	13N/02	granitic gneiss	KIS	5.17	1.05	0.1232	0.511345	-0.3738	-25.2	0.509028	0.508937	2893
16	18CXAD041A1	N/A	663587	6165625	13N/09	gneissic granodiorite	MG	15.72	2.74	0.1053	0.510768	-0.4646	-36.5	0.508506	0.508412	3248
17	18CXAD042A1	N/A	664156	6162966	13N/09	gneissic granodiorite	MG	14.61	2.77	0.1147	0.511007	-0.4171	-31.8	0.508544	0.508412	3181
18	18CXAD056B	N/A	629285	6147622	13N/07	foliated granodiorite	KIS	11.70	1.57	0.0809	0.510590	-0.5887	-40.0	0.509068	0.508937	2840

Notes: All coordinates are in NAD27 datum, zone 20. Ref#s in red were analyzed at Carleton University. Abbreviations: HRB=Hunt River belt; WA=Weekes Amphibolite; WU=Weekes ultramafic; KIS=Kanairiktok Intrusive Suite; MG=Maggo Gneiss

Technologies, LLC, USA). The Sr fractions were loaded on the columns and were washed in 1.6 ml of 7M HNO₃. Sr was eluted in 1.6 ml of ultra-pure water. The Sr, Sm and Nd isotope ratios were measured using IGGRC's Thermo-Finnigan Neptune MC-ICP-MS. The Sr and Nd isotopic ratios were normalized against ⁸⁶Sr/⁸⁸Sr=0.1194 and ¹⁴⁶Nd/¹⁴⁴Nd= 0.7219, respectively.

The average values of bracketing standard reference materials for a period of six months covering this analysis session are NBS987 ⁸⁷Sr/⁸⁶Sr = 0.710239 ± 0.000019 (2SD, n=43) and JNdi-1 ¹⁴³Nd/¹⁴⁴Nd = 0.512093 ± 0.000015 (2SD, n=52). The total procedure blanks are <250 pg and <50 pg for Sr and Nd, respectively.

LITHOGEOCHEMICAL RESULTS

ALTERATION, METAMORPHISM AND ELEMENT MOBILITY

The Weekes Amphibolite and Hunt River Belt rocks were metamorphosed to amphibolite-varying to granulite-facies mineral assemblages. Both units commonly exhibit rusty patches and planar zones containing elevated pyrrhotite and pyrite. Many samples of the Weekes Amphibolite and Hunt River Belt amphibolite lie above the "fresh basalt" field and have an elevated CCPI alteration index, suggesting Mg-Fe carbonate alteration (Large *et al.*, 2001; *see* Figure 4). The Weekes ultramafic rocks also lie above the "fresh basalt" field and project toward the chlorite+pyrite apex as they are enriched in FeO^T and, in particular MgO. Because of their antiquity, high metamorphic grade and field evidence for alteration, the immobile trace elements (high-field strength (HFSE) and rare-earth (REE) elements), essentially immobile under most fluid – rock interactions (*e.g.*, Pearce and Cann 1973; Wood *et al.*, 1980; Middelburg *et al.*, 1988), are emphasized for petrological and geotectonic interpretations.

CLASSIFICATION, AND MAJOR- AND TRACE-ELEMENT VARIATIONS

Although all samples of the Hunt River Belt and the Weekes Amphibolite were termed amphibolite in the field, they exhibit a wide range of SiO₂ (45.3 to 68.3 wt. %), low but variable total alkalis, and are subalkaline basalt

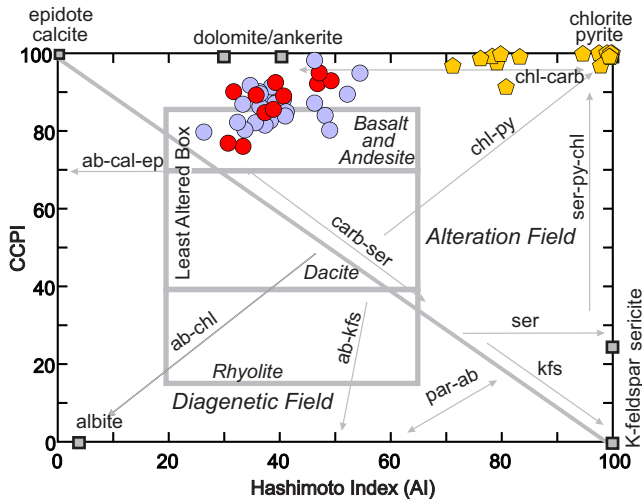


Figure 4. Alteration box plot illustrating the CCPI (chlorite-carbonate-pyrite index) vs. the AI (Alteration Index) as per Large et al. (2001).

ranging to dacite (Figure 5A). The Weekes ultramafic rocks similarly exhibit a wide range of SiO₂ (35.3 to 56.8 wt. %) and low, variable total alkalis and are picrobasalt ranging to andesite (Figure 5A). The Weekes ultramafic rocks are komatiite with one sample having elevated alkalis and plotting above the komatiite-meimechite field, likely reflecting alteration (Figure 5B). The the Hunt River Belt and Weekes Amphibolite are picrobasalt ranging to basalt (Figure 5B). Immobile trace-element plots illustrate that both the Hunt River Belt and the Weekes Amphibolite samples are subalkaline tholeiitic basalts (Figure 5C, D).

The collective major- and compatible trace-element chemistry of the rocks are outlined in major element vs. Mg# (molecular (MgO/MgO+FeO^T)*100) diagrams (Figure 6). Collectively, they demonstrate that the rocks of the Hunt River Belt and Weekes Amphibolite exhibit broadly similar fractionation trends in terms of all elements vs. fractionation index (Mg#). The SiO₂, Al₂O₃ and CaO vary little with

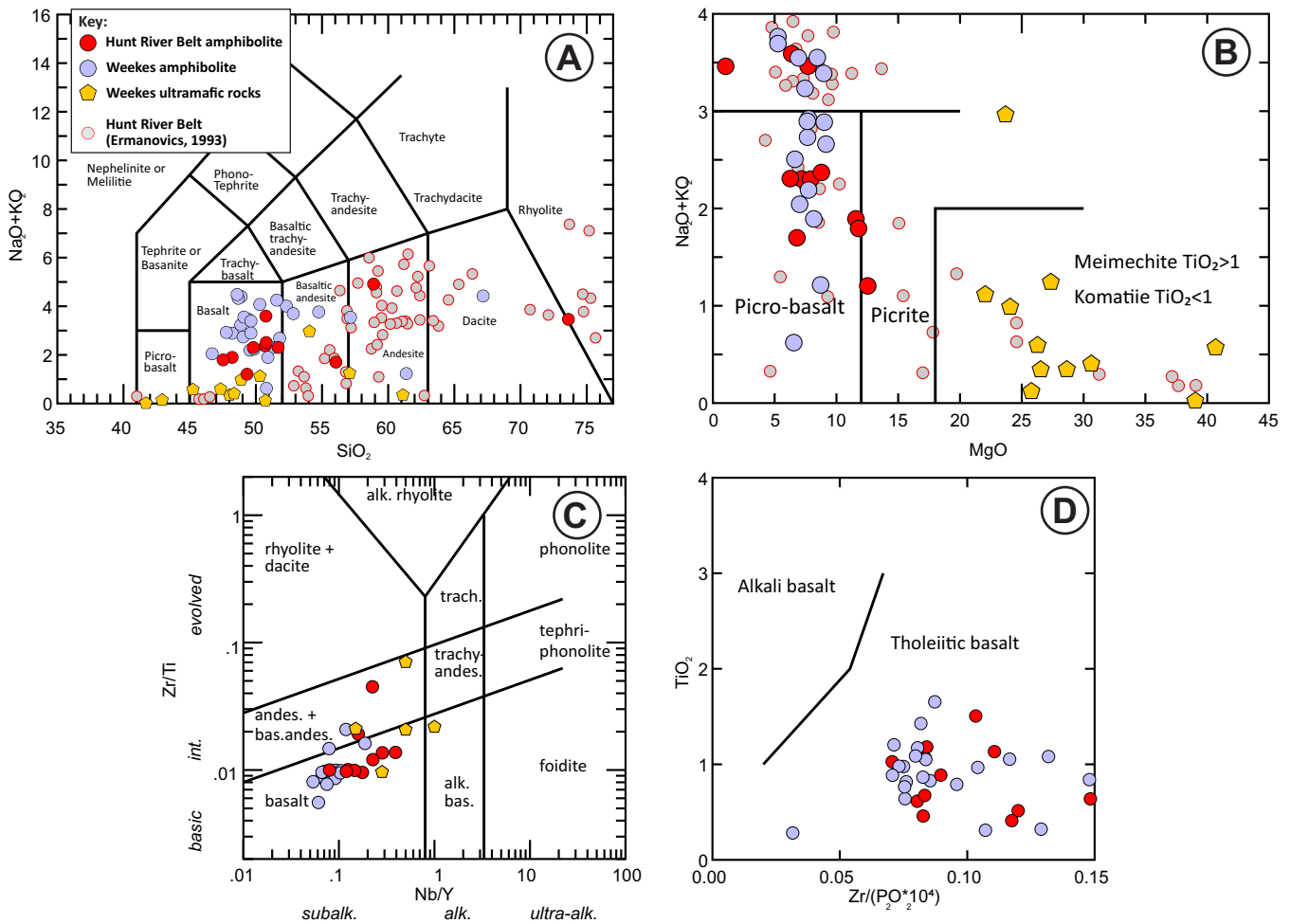


Figure 5. Classification diagrams for rocks of the Hunt River Belt and Weekes Amphibolite. A) TAS diagram (LeMaitre, 1989); B) High-MgO TAS diagram (LeMaitre et al., 2004); C) Zr/Ti vs. Nb/Y (Pearce, 1996); D) TiO₂ vs. Zr/(P₂O₅*10⁴) (Winchester and Floyd, 1976).

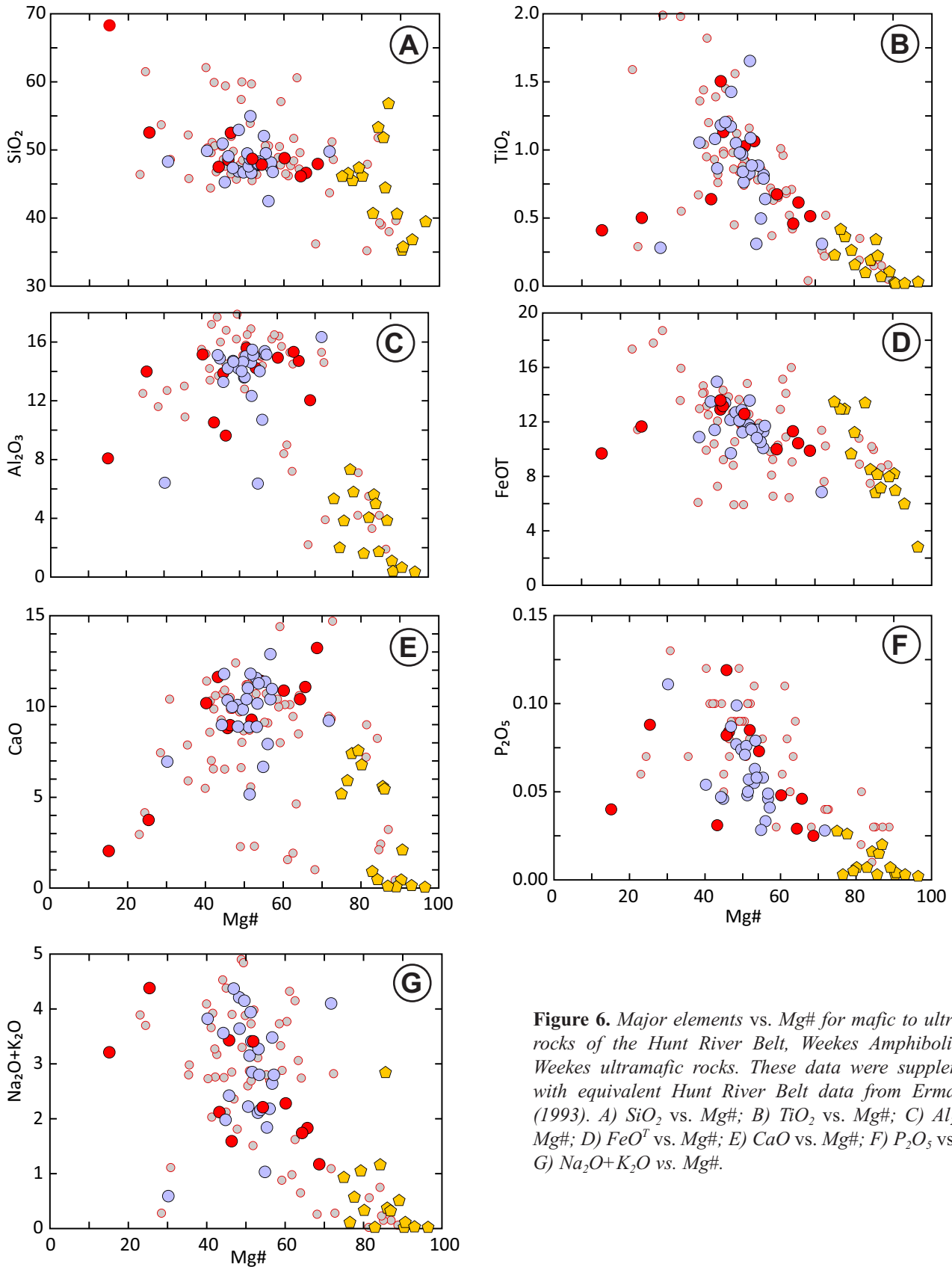


Figure 6. Major elements vs. Mg# for mafic to ultramafic rocks of the Hunt River Belt, Weekes Amphibolite and Weekes ultramafic rocks. These data were supplemented with equivalent Hunt River Belt data from Ermanovics (1993). A) SiO₂ vs. Mg#; B) TiO₂ vs. Mg#; C) Al₂O₃ vs. Mg#; D) FeO^T vs. Mg#; E) CaO vs. Mg#; F) P₂O₅ vs. Mg#; G) Na₂O+K₂O vs. Mg#.

increasing fractionation, whereas FeO^T increases modestly. In contrast, TiO_2 , P_2O_5 , Na_2O and K_2O increase with increasing fractionation (Figure 6). The mantle compatible elements Cr, Ni and Co all decrease with increasing fractionation whereas Sc and V increase with fractionation (Figure 7).

REE AND MULTI-ELEMENT PLOTS

Hunt River Belt amphibolites exhibit flat to weakly LREE-enriched and LREE-depleted rare-earth-element pat-

terns ($(\text{La}/\text{Sm})_{\text{CN}} = 0.15\text{--}2.02$: Figure 8A) typically with elemental abundances between 6 and 50 times chondrite. These are broadly similar overall to those for the Weekes Amphibolite (Figure 8B) that have $(\text{La}/\text{Sm})_{\text{CN}} = 0.13\text{--}4.14$ ranging from 5 to 35 times chondrite. Both units have overlapping, weakly positive Eu anomalies, with the Hunt River Belt samples having $\text{Eu}/\text{Eu}^* = 1.85\text{--}2.75$ compared to 1.82–2.74 for the samples of Weekes Amphibolite. Weekes ultramafic rocks have low concentrations of the rare-earth elements, many of which are below detection, and therefore

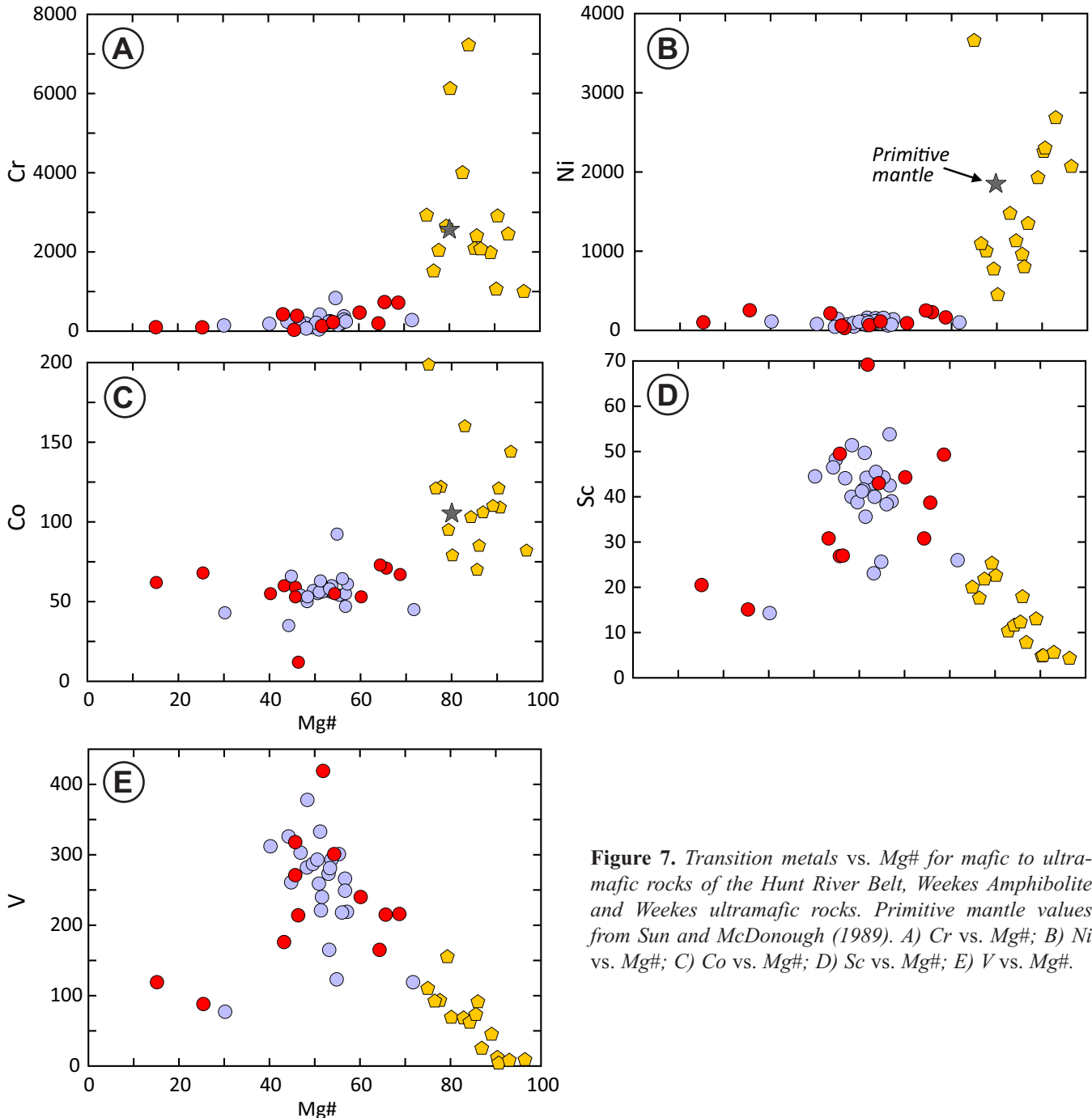


Figure 7. Transition metals vs. Mg# for mafic to ultramafic rocks of the Hunt River Belt, Weekes Amphibolite and Weekes ultramafic rocks. Primitive mantle values from Sun and McDonough (1989). A) Cr vs. Mg#; B) Ni vs. Mg#; C) Co vs. Mg#; D) Sc vs. Mg#; E) V vs. Mg#.

exhibit jagged, broadly flat REE profiles generally <10x chondrite (Figure 8C).

The Hunt River Belt amphibolites have generally flat, ranging from weakly LILE and LREE-enriched to weakly LILE and LREE-depleted multi-element patterns commonly having minor Nb, P and Ti troughs (Figure 9A). The elements typically range in abundance from 2 to 20x primitive

mantle. The LILE and LREE-depleted and enriched samples occur proximal to one another in the same outcrop areas (e.g., samples 19HS40B vs. 19HS40C). The Weekes Amphibolite samples are similar to the Hunt River Belt amphibolites and have generally flat, ranging to weakly LILE and LREE-enriched and depleted multi-element patterns commonly with minor Nb, P and Ti troughs (Figure 9B). The elements typically range in abundance from 1 to

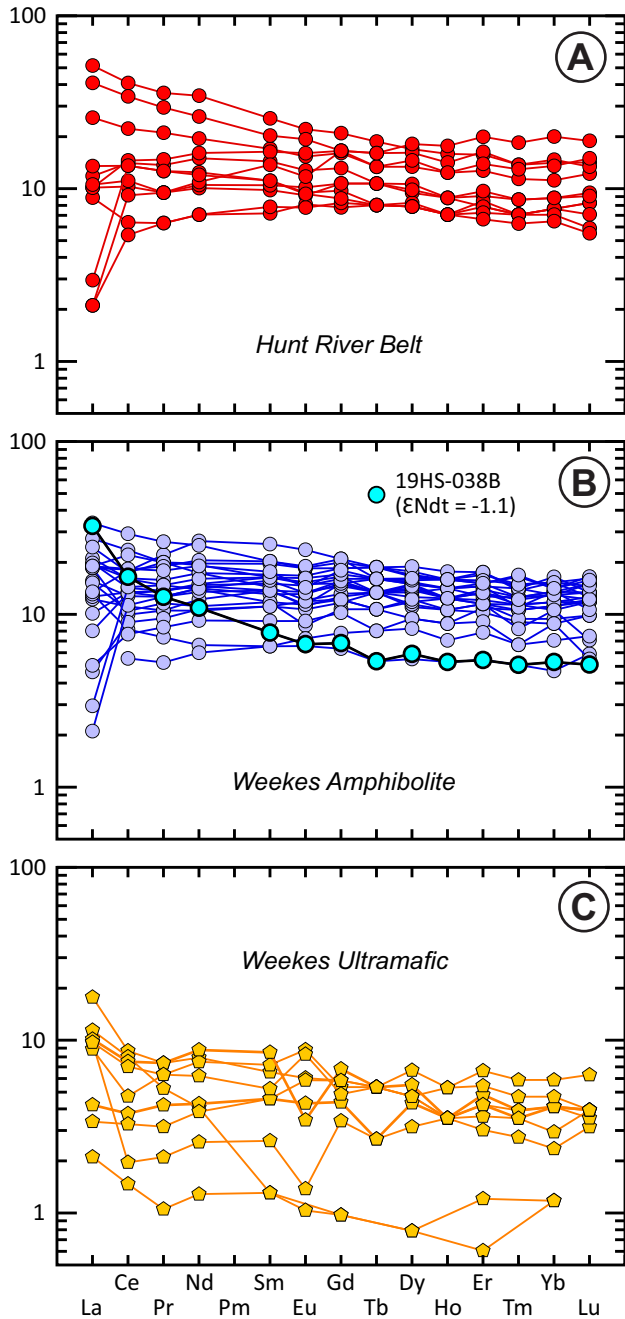


Figure 8. Chondrite normalized rare-earth element diagrams (Sun and McDonough, 1989) for rocks of: A) Hunt River Belt; B) Weekes Amphibolite mafic and; C) Weekes Amphibolite ultramafic rocks.

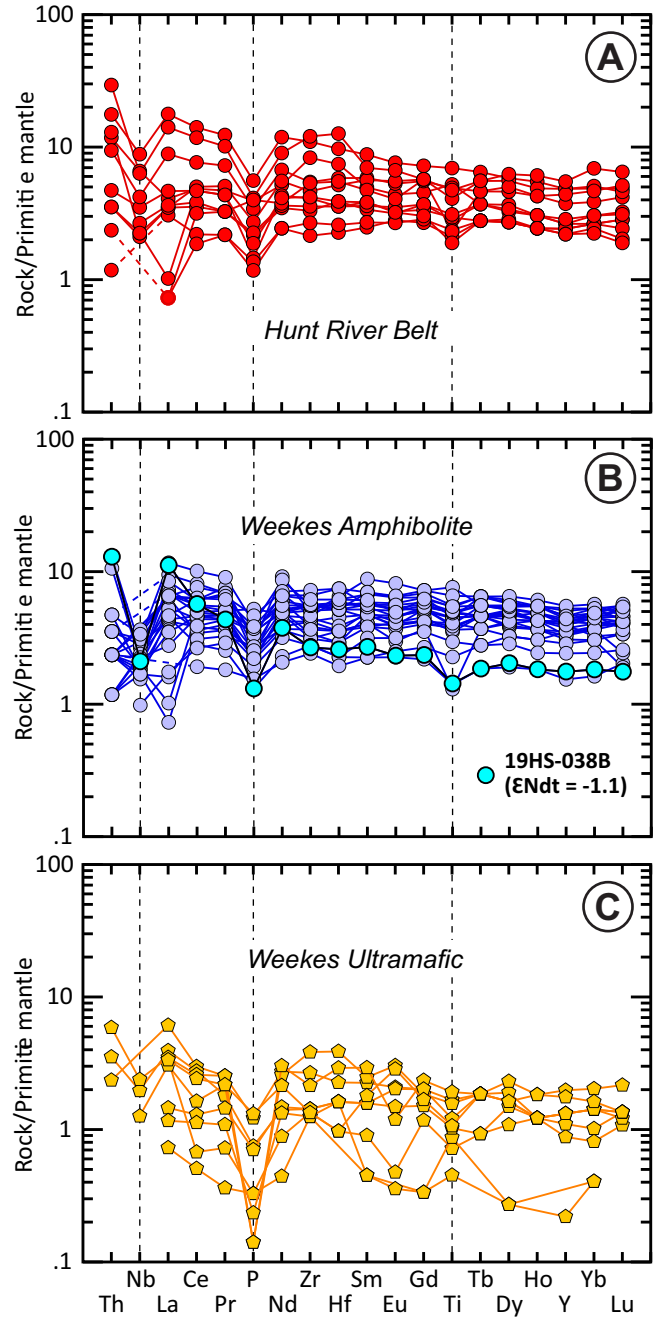


Figure 9. Multi-element plots normalized to primitive mantle (Sun and McDonough, 1989) for rocks of: A) Hunt River Belt; B) Weekes Amphibolite mafic and; C) Weekes Amphibolite ultramafic rocks.

10x primitive mantle. The Weekes ultramafic rocks have low concentrations of incompatible trace elements, many of which are below detection, and exhibit jagged, broadly flat multi-element profiles that typically range in abundance from <1 to 6x primitive mantle (Figure 9C).

Nd ISOTOPES

All ϵNd_t values for the amphibolites are recalculated to $t=3100$ Ma (DePaolo, 1981; Table 2; Figure 10). The 2 samples of Maggo Gneiss were recalculated to $t=3250$ Ma and the 2 samples of the Kanairiktok Intrusive Suite were recalculated to $t=2850$ Ma. All specimens of the Hunt River Belt yield present-day $^{144}\text{Nd}/^{143}\text{Nd}$ ratios ranging from 0.511865 to 0.513156, corresponding to $\epsilon Nd_{t=3100}$ Ma values of +1.4 to +2.4 (mean = +1.9; $n = 3$, Table 2; Figure 10). The Weekes Amphibolite samples in comparison exhibit present-day $^{144}\text{Nd}/^{143}\text{Nd}$ ratios ranging from 0.511576 to 0.513008, corresponding to $\epsilon Nd_{t=3100}$ Ma values of -1.1 to

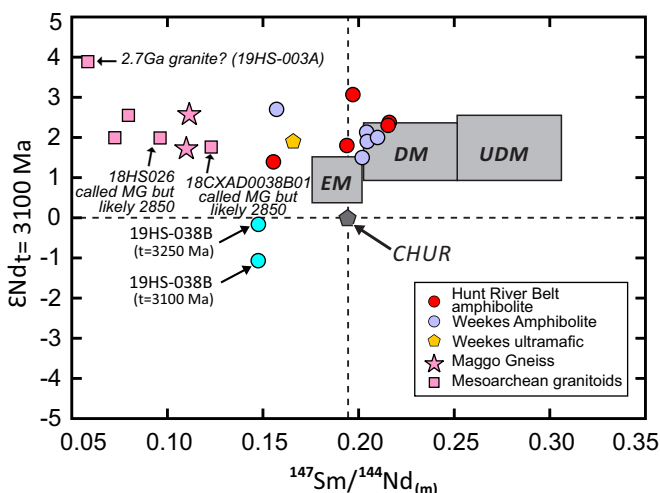


Figure 10. $\epsilon Nd_{t=3100}$ Ma vs. $^{147}\text{Sm}/^{144}\text{Nd}$ for selected rocks of the Hunt River Belt and Weekes Amphibolite compared to fields for approximated ultra-depleted mantle (UDM), depleted mantle (DM), enriched mantle (EM) and the Chondritic uniform Reservoir (CHUR) using the depleted mantle growth curve of DePaolo (1981). Also shown are geochronologically constrained (Rayner, 2022) samples of tonalitic Maggo Gneiss ($n=2$: recalculated at $t=3250$ Ma) and Kanairiktok granitoid rocks ($n=2$: recalculated at $t=2850$ Ma). Two samples of gneissose tonalite inferred to be Maggo Gneiss have $\epsilon Nd_{t=3250}$ Ma greater than contemporaneous depleted mantle and are more reasonably interpreted as ca. 2850 Ma Kanairiktok granitoid gneisses. One other sample, interpreted as Kanairiktok Intrusive Suite, yields an $\epsilon Nd_{t=2850}$ Ma of 4, higher than contemporaneous depleted mantle and suggesting the rock may be ca. younger than 2850 Ma.

+3.1 (mean = +1.7; $n = 7$, Table 2; Figure 10). These data generally overlap, within error, the value for contemporaneous depleted mantle (DM), their mean value is identical to that for DM ($\text{DM}_{t=3100 \text{ Ma}} = +1.6$; DePaolo, 1981) and the standard deviation comparable to the calculated analytical, 2σ standard deviation of 0.5–0.8 ϵ units.

DISCUSSION

Previous investigators (Ermanovics and Raudsepp, 1979; Ermanovics *et al.*, 1982; Finn, 1989a, b, 1991; Ermanovics, 1993) interpreted the Hunt River Belt as the oldest intact unit in the region, and all other supracrustal rafts of amphibolite, metasedimentary and ultramafic units engulfed by gneissic and intrusive rocks (Maggo Gneiss, Kanairiktok Intrusive Suite) were termed Weekes Amphibolite (units A'Wab and A'Wan, Ermanovics, 1993). They interpreted these rafts to represent, at least in part, the dismembered remnants of the Hunt River Belt. Concurrently, and based on imprecise, whole-rock Rb–Sr isochron data, Finn (1989a, b, 1991) and Ermanovics (1993), indicated that the components of the Maggo Gneiss ranged in age from ca. 3300 to 3100 Ma, in part contemporaneous with the Hunt River Belt.

James *et al.* (2002) provided the first documented zircon age for the tonalitic component of the Maggo Gneiss, yielding a poorly constrained TIMS U–Pb zircon age of ca. 3250 Ma. Recent sensitive high-resolution ion microprobe (SHRIMP) U–Pb geochronology (Rayner, 2022) has confirmed the antiquity of the Maggo Gneiss and 3 new ages from a number of widely separated localities of tonalitic gneiss yield a range from 3260–3250 Ma, further illustrating the age of the precursor igneous intrusions of the gneiss. These ages correlate well with the single, poorly constrained age of 3258 ± 24 Ma age for Weekes metasedimentary, low-U detrital zircons from a sample from the Hopedale Block (Schjøtte *et al.*, 1989) and suggest that some of the supracrustal rafts, screens and boudins (Weekes Amphibolite) form part of the Maggo Gneiss *sensu stricto*. This suggestion supports that of Loveridge *et al.* (1987) and James *et al.* (2002), the latter outlined a time evolutionary sequence for the Hopedale Block different from previous interpretations (*viz.* Ermanovics, 1993; Wasteneys *et al.*, 1996), and proposed that some of the Weekes Amphibolite represents a supracrustal component older than, or comparable in age to, the Maggo Gneiss. Clearly, the possibility exists that the amphibolitic remnants preserved in the Maggo Gneiss and Kanairiktok Intrusive Suite likely represent both early, Maggo Gneiss age-equivalent amphibolite as well as engulfed remnants of the Hunt River Belt, and perhaps even the Florence Lake Belt.

IMPLICATIONS OF THE NEW DATA

The new lithochemical and Nd isotopic data, along with compiled historical data, show that Hunt River Belt and Weekes Amphibolite are broadly very similar. Both represent suites of sub-alkaline tholeiitic basalts to picritic basalts. Major- and compatible trace-element variation trends versus Mg#, for both types of amphibolites reflect the dominant crystallization of magnesian olivine + orthopyroxene with minor clinopyroxene. Olivine and orthopyroxene both have relatively high mineral/melt distribution coefficients for Cr, Ni and Co, but lower distribution coefficients for Sc and V (Rollinson, 1993; McDade *et al.*, 2003). It is unlikely significant amounts of clinopyroxene were removed from the melts as CaO remains relatively constant over ~30 Mg# units and Sc and V increase with fractionation (Figures 6 and 7). It is similarly unlikely spinel was part of the crystallization sequence for the amphibolites as TiO₂ and V increase with fractionation and these elements are strongly fractionated into spinel. Moreover, concentrations of Cr and Ni are low, an indication that if spinel had been on the liquidus, it must have been early in the petrogenesis of these rocks.

Although broadly very similar in terms of their major- and compatible trace-element abundances, the incompatible trace elements and trace-element ratios outline some clear distinctions (Figure 11). The Hunt River Belt amphibolites have higher Nb/Yb, Zr/Y and Nb/Y ratios than the Weekes Amphibolite samples (Figure 11A, B). Although having similar trends toward the Th apex, and perhaps implying “arc” magmatic series, the two types of amphibolite define trends toward different Th-poor mantle sources (Figure 11C). Figure 11D–F similarly distinguish the two types of amphibolite. The Hunt River Belt rocks plot between the NMORB and EMORB fields on many tectonic discrimination diagrams, whereas the Weekes Amphibolite samples plot largely in the NMORB field. Collectively, their trace elements indicate that the Hunt River Belt amphibolites were derived from a slightly more enriched mantle source, although both units appear to range from LREE-depleted to slightly enriched varieties with variable minor HFSE troughs suggesting some recycling of the lithosphere. The Nd isotopic values overlap extensively with depleted mantle at 3100 Ma, indicating that most amphibolites, either from the Hunt River Belt or from the Weekes Amphibolite, were derived from mantle sources of similar antiquity, and if lithospheric contamination occurred, then the contaminant was of comparable age as the amphibolite’s parental basaltic magmas.

Only one specimen of the Weekes Amphibolite (19HS-038B) yielded an $\epsilon\text{Nd}_{t=3100}$ Ma < 1 (-1.1), is LREE-enriched

and also has the most prominent negative Nb anomaly. Collectively, these features suggest that this sample exhibits the best evidence for containing a slightly older lithospheric/subduction component in its genesis. One sample is not conclusive, but this suggests that at least some of the Weekes Amphibolite samples may represent older, Maggo Gneiss – affiliated amphibolite. This, along with their somewhat differing compositions, suggest that both older Maggo Gneiss – affiliated amphibolite, and younger dispersed remnants of the Hunt River and Florence Lake belts components are represented in the Weekes Amphibolite. Documentation of the field and geochronological relationships between the enclosing granitoid rocks and the amphibolites is critical for further understanding of the early history of the Hopedale Block.

The Weekes ultramafic rocks occur as metamorphosed rafts in granitic rocks and preserve no primary textures, in particular spinifex, so they are better referred to as picrites or harzburgites (*see* Kerr and Arnt, 2001). The Weekes ultramafic rocks have relatively low abundances of all elements except MgO, SiO₂, FeOT, Cr, Ni and Co. They are picrobasalt ranging to komatiite or harzburgite. Their incompatible trace-element abundances are low, commonly close to the detection limit of the analytical methods and further study of their origin requires alternative low-level trace-element analyses.

CONCLUSIONS

1. Major- and compatible trace-element abundances of the Weekes Amphibolite and Hunt River Belt amphibolites are broadly similar and both comprise subalkaline, tholeiitic basaltic rocks.
2. The incompatible trace elements and trace-element ratios, however, indicate that Hunt River Belt amphibolites have higher Nb/Yb, Zr/Y and Nb/Y than the Weekes Amphibolite samples.
3. Hunt River Belt amphibolites were largely derived from a slightly more enriched mantle source.
4. Although the Nd isotopic characteristics of the two suites are very similar and overlap the value for corresponding depleted mantle, one sample of Weekes Amphibolite yielded an $\epsilon\text{Nd}_{t=3100}$ Ma = -1.1, with corresponding LREE-enrichment and HFSE troughs; thereby suggesting some recycling of crust older than the Maggo Gneiss, or older, unrecognized parts of the Maggo Gneiss.

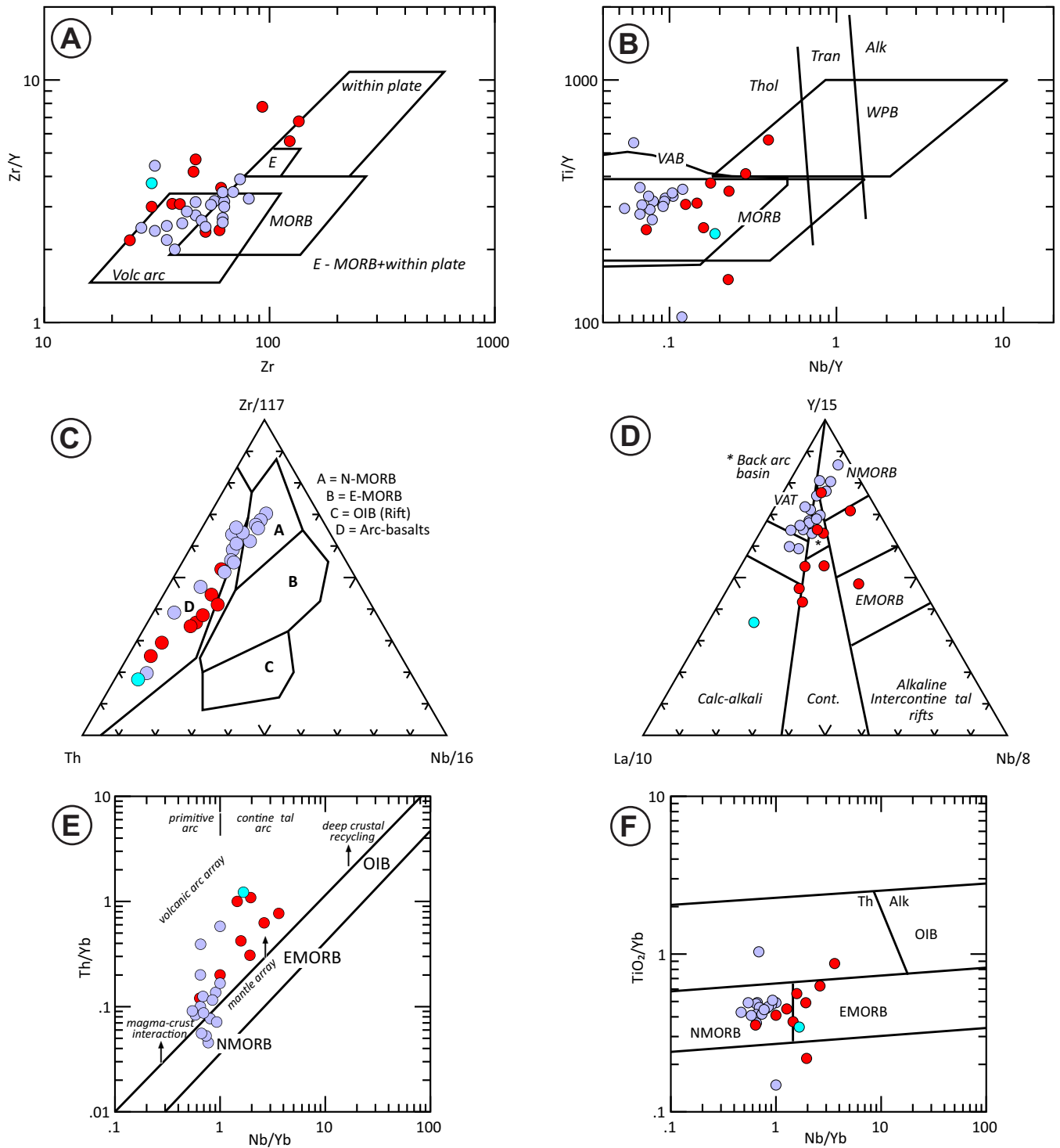


Figure 11. Trace-element geotectonic discrimination diagrams for basaltic rocks of the Hunt River Belt and Weekes Amphibolite. A) Zr/Y vs. Zr (Pearce and Norry, 1979); B) Ti/Y vs. Nb/Y (Pearce, 1982); C) Th-Zr/117-Nb/16 diagram (Wood et al., 1980). D) La/10-Y/15-Nb/8 diagram (Cabanis and Lecolle, 1989); E) Th/Yb vs. Nb/Y (Pearce, 2008); F) TiO₂/Yb vs. Nb/Yb (Pearce, 2008).

5. The lithochemical and Nd isotopic data for the Weekes Amphibolite and Hunt River Belt amphibolite support two distinct mafic magmatic events in the Hopedale Block at >3200 Ma and at *ca.* 3100 Ma, respectively.

ACKNOWLEDGMENTS

H. Sandeman gratefully acknowledges the exuberant field assistance of Alex Bugden and Tyler Nickson as well as Hopedale prospector Edmund Saunders and associates who were instrumental in sharing local knowledge of the region and the rocks of the Hopedale area and welcomed us into the community. Fieldwork also benefitted from the knowledge of Arverktok (Hopedale) community members Shevonne Tuglavina, Allan Pijogge, Albert Tuglavina and Patty Dicker. Canadian Helicopter Services provided excellent helicopter support. This research was conducted, in part, on Labrador Inuit Lands with permission of the Nunatsiavut Government, NGRAC-19577773. Charmaine Hamlyn and Kim Morgan are thanked for their cartographic support.

REFERENCES

- Bridgwater, D. and Schiøtte, L.
1991: The Archaean gneiss complex of northern Labrador: A review of current results, ideas and problems. *Bulletin of the Geological Society Denmark*, Volume 39, pages 153-166. <https://doi.org/10.37570/bgsd-1991-39-06>.
- Bridgwater, D., Watson, J. and Windley, B.F.
1973: The Archaean craton of the North Atlantic region. *Philosophical Transactions of the Royal Society of London*, Volume 273, pages 493-512.
- Brooks, C.
1982: Third report on the geochronology of Labrador pertaining to sub-project 109. Government of Newfoundland and Labrador, Department of Mines and Energy, Mineral Development Division, Open File Labrador 519.
1983: U-Pb geochronological ages. A report to Energy Mines and Resources concerning contract No. 1. EMP-MMD-82-0052 and amendment No. 1. Open File Labrador 519.
- Cabanis, B. and Lecolle, M.
1989: Le diagramme La/10-Y/15-Nb/8: un outil pour la discrimination des series volcaniques et la mise en evidence des processus de melange et/ou de contamination crustale. *Comptes Rendus de l'Academie des Sciences, Series II*, Volume 309, pages 2023-2029.
- Cadman, A.C., Heaman, L., Tarney, J., Wardle, R. and Krogh, T.E.
1993: U-Pb geochronology and geochemical variation within two Proterozoic mafic dyke swarms, Labrador. *Canadian Journal of Earth Sciences*, Volume 30, pages 1490-1504.
- Coyle, M.
2019: Residual total magnetic field, aeromagnetic survey of the Hopedale area, Newfoundland and Labrador, part of NTS 13-N/north. Geological Survey of Canada, Open File 8514, 1 sheet. <https://doi.org/10.4095/313296>
- DePaolo, D.J.
1981: Neodymium isotopes in the Colorado Front Range and crust-mantle evolution in the Proterozoic. *Nature*, Volume 291, pages 193-196.
- Ducharme, T.A., McFarlane, C.R.M., van Rooyen, D. and Corrigan, D.
2021: Petrogenesis of the peralkaline Flowers River Igneous Suite and its significance to the development of the southern Nain Batholith. *Geological Magazine*, Volume 158, pages 1911-1936. DOI: <https://doi.org/10.1017/S0016756821000388>
- Emslie, R.F.
1980: Geology and petrology of the Harp Lake Complex, central Labrador: An example of Elsonian magmatism. *Geological Survey of Canada, Bulletin* 293.
- Ermanovics, I.
1993: Geology of Hopedale Block, southern Nain Province, and the adjacent Proterozoic terranes, Labrador, Newfoundland. Geological Survey of Canada, Memoir 431, 161 pages.
- Ermanovics, I.F., Korstgård, J.A. and Bridgwater, D.
1982: Structural and lithological chronology of the Archean Hopedale block and the adjacent Proterozoic Makkovik Subprovince, Labrador; Report 4. *In Current Research, Part B*. Geological Survey of Canada, Paper 82-IB, pages 153-165.
- Ermanovics, I. and Raudsepp, M.
1979: Geology of the Hopedale Block of eastern Nain Province, Labrador: Report 1. *In Current Research, Part B*. Geological Survey of Canada, Paper 79-1B, pages 341-348.

- Finch, C., Roldan, R., Walsh, L., Kelly, J. and Amor, S.
2018: Analytical methods for chemical analysis of geological materials. Government of Newfoundland and Labrador, Department of Natural Resources, Geological Survey, Open File NFLD/3316, 67 pages.
- Finn, G.C.
1989a: Geochemical and isotopic evolution of the Maggo gneiss component from the Hopedale Block, Labrador: Evidence for Late - Middle Archaean crustal reworking. Ph.D. thesis, Memorial University of Newfoundland, St. John's, Newfoundland and Labrador.

1989b: Rb-Sr geochronology of the Archaean Maggo gneiss from the Hopedale Block, Nain Province, Labrador. *Canadian Journal of Earth Sciences*, Volume 26, pages 2512-2522.

1991: Major-, trace-, and rare-earth-element geochemistry of the Archaean Maggo gneisses, southern Nain Province, Labrador. *Canadian Journal of Earth Sciences*, Volume 28, pages 44-57.
- Hill, J.D.
1982: Geology of the Flowers River – Natakwanon River area, Labrador. Government of Newfoundland and Labrador, Department of Mines and Energy, Mineral Development Division, Report 82-6, 140 pages.
- Hinchey, A.M., Diekrup, D. and Rayner, N.
2023: Revisiting Mesoproterozoic magmatism in Labrador: Evaluating AMCG and peralkaline magmatism. *In Current Research*. Government of Newfoundland and Labrador, Department of Industry, Energy and Technology, Geological Survey, Report 23-1, pages 1-16.
- Hinchey, A.M., Sandeman, H.A. and Campbell, H.E.
2021: Geochemical data from the Hopedale Block (NTS map areas 13M and 13N), Labrador. Government of Newfoundland and Labrador, Department of Industry, Energy and Technology, Geological Survey, Open File LAB/1763, 8 pages.
- James, D.T.
1997: The Archaean Hunt River greenstone belt, Hopedale Block, eastern Labrador (NTS 13N/7 and 13N/10): Geology and exploration potential. *In Current Research*. Government of Newfoundland and Labrador, Department of Mines and Energy, Geological Survey, Report 97-1, pages 9-27.
- James, D.T., Kamo, S. and Krogh, T.
2002: Evolution of 3.1 and 3.0 Ga volcanic belts and a new thermotectonic model for the Hopedale Block, North Atlantic craton (Canada). *Canadian Journal of Earth Sciences*, Volume 39, pages 687-710.
- James, D.T., Miller, R.R., Patey, R.P. and Thibodeau, S.
1996: Geology and mineral potential of the Archaean Florence Lake greenstone belt, Hopedale Block (Nain Province), eastern Labrador. *In Current Research*. Government of Newfoundland and Labrador, Department of Natural Resources, Geological Survey, Report 96-1, pages 85-107.
- Jesseau, C.W.
1976: A structural, metamorphic and geochemical study of the Hunt River supracrustal belt, Nain Province, Labrador. Unpublished M.Sc. thesis, Memorial University of Newfoundland, St. John's, Newfoundland and Labrador, 211 pages.
- Kerr, A.C. and Arndt, N.T.
2001: A note on the IUGS reclassification of the high-Mg and picritic volcanic rocks. *Journal of Petrology*, Volume 42, pages 2169-2171. <https://doi.org/10.1093/petrology/42.11.2169>
- Korstgård, J.A. and Ermanovics, I.F.
1985: Tectonic evolution of the Archaean Hopedale Block and the adjacent Makkovik subprovince, Labrador, Newfoundland. *In Evolution of Archaean Supracrustal Sequences*. Edited by L.D. Ayres, P.C. Thurston, K.D. Card and W. Weber. Geological Association of Canada, Special Paper 28, pages 223-237.
- Krogh, T.E.
1992: Report on 1992 geochronological contract work, Labrador. Unpublished report to Newfoundland Department of Mines and Energy. Government of Newfoundland and Labrador, Department of Mines and Energy, Geological Survey Branch, 69 pages. Open File Lab 944. [2229-2240, 2249-2257].

1993: Report on Labrador geochronology, 1992-93. Government of Newfoundland and Labrador, Department of Mines and Energy, Geological Survey Branch, Open File Labrador 997.

- Le Maitre, R.W. (Editor), Streckeisen, A., Zanettin, B., Le Bas, M.J., Bonin, B., Bateman, P., Bellieni, G., Dudek, A., Efremova, S., Keller, J., Lameyre, J., Sabine, P.A., Schmid, R., Sørensen, H. and Woolley, A.R.
2004: *Igneous Rocks: A Classification and Glossary of Terms*. Cambridge University Press, The Edinburgh Building, Cambridge, United Kingdom, CB2 2RU.
- Loveridge, W.D., Ermanovics, I.F. and Sullivan, R.W.
1987: U–Pb ages on zircon from the Maggo gneiss, the Kanairiktok Plutonic Suite, coast of Labrador, Newfoundland. Geological Survey of Canada, Paper 87-2, pages 59-65.
- McDade, P., Blundy, J.D. and Wood, B.J.
2003: Trace element partitioning between mantle wedge peridotite and hydrous MgO-rich melt. *American Mineralogist*, Volume 88, pages 1825-1831.
- Pearce, J.A.
1982: Trace element characteristics of lavas from destructive plate boundaries. *In Organic Andesites and Related Rocks*. Edited by R.S. Thorpe. John Wiley and Sons, Chichester, England, pages 528-548.

1996: A user's guide to basalt discrimination diagrams. *In Trace Element Geochemistry of Volcanic Rocks; Applications for Massive Sulphide Exploration*. Short Course Notes, Geological Association of Canada, Volume 12, pages 79-113.

2008: Geochemical fingerprinting of oceanic basalts with applications to ophiolite classification and the search for Archean oceanic crust. *Lithos*, Volume 100, pages 14-48. <https://doi.org/10.1016/j.lithos.2007.06.016>
- Pearce, J.A. and Norry, M.J.
1979: Petrogenetic implications of Ti, Zr, Y, and Nb variations in volcanic rocks. *Contributions to Mineralogy and Petrology*, Volume 69, pages 33-47. <https://doi.org/10.1007/BF00375192>
- Rayner, N.M.
2022: Report on U–Pb geochronology from the 2017–2020 GEM-2 activity “Saglek Block, Labrador: Geological evolution and mineral potential”. Geological Survey of Canada, Open File 8901. <https://doi.org/10.4095/330237>.
- Rollinson, H.R.
1993: *Using Geochemical Data: Evaluation, Presentation, Interpretation*. London, Longman Scientific and Technical, ISBN 0 58206701 4, 352 pages.
- Sahin, T. and Hamilton, M.A.
2019: New U–Pb baddeleyite ages for Neoproterozoic and Paleoproterozoic mafic dyke swarms of the southern Nain Province, Labrador: Implications for possible plate reconstructions involving the North Atlantic craton. *Precambrian Research*, Volume 329, pages 44-69.
- Sandeman, H.A.I. and McNicoll, V.J.
2015: Age and petrochemistry of rocks from the Aucoin gold prospect (NTS map area 13N/6), Hopedale Block, Labrador: Late Archean, alkali monzodiorite–syenite hosts Proterozoic orogenic Au–Ag–Te mineralization. *In Current Research*. Government of Newfoundland and Labrador, Department of Natural Resources, Geological Survey, Report 15-1, pages 85-103.
- Sandeman, H.A. and Rafuse, H.
2011: The geological setting of Au–Ag–Te mineralization at the Aucoin prospect (NTS 13N/6) Hopedale Block, Labrador. *In Current Research*. Government of Newfoundland and Labrador, Department of Natural Resources, Geological Survey, Report 11-1, pages 167-183.
- Schiøtte, L., Compston, W. and Bridgwater, D.
1989: Ion probe U–Th–Pb zircon dating of polymetamorphic orthogneisses from northern Labrador, Canada. *Canadian Journal of Earth Sciences*, Volume 26, pages 1533-1556.
- Sparkes, G.W., Dunning, G.R. and McNicoll, V.J.
2010: New U–Pb age constraints and potential implications for the genesis of the Kitts uranium deposit, Central Mineral Belt, Labrador. *In Current Research*. Government of Newfoundland and Labrador, Department of Natural Resources, Geological Survey, Report 10-1, pages 93-109.
- Sun, S.S. and McDonough, W.F.
1989: Chemical and isotopic systematics of oceanic basalts: Implications for mantle composition and processes. *In Magmatism in the Ocean Basin*. Edited by A.D. Saunders and M.J. Norry. Geological Society of London, Special Publication 42, pages 313-345.
- Taylor, F.C.
1977: *Geology, Hopedale, Newfoundland*. Map 1443A. Scale: 1:250 000. Geological Survey of Canada. Colour map. GS# 013N/0009.

- 1979: Reconnaissance geology of a part of the Precambrian Shield. northeastern Quebec, northern Labrador and Northwest Territories: Geological Survey of Canada, Memoir 393, 99 pages.
- Tanaka, T., Togashi, S., Kamioka, H., Amakawa, H., Kagami, H., Hamamoto, T., Yuhara, M., Orihashi, Y., Yoneda, S., Shimizu, H., Kunimaru, T., Takahashi, K., Yanagi, T., Nakano, T., Fujimaki, H., Shinjo, R., Asahara, Y., Tanimizu, M., Dragusanu, C.
2000: JNdi-1: A Neodymium isotopic reference in consistency with LaJolla Neodymium. *Chemical Geology*, Volume 168, pages 279-281.
- Tettelaar, T. A.
2004: Emplacement history of the Pearly Gates anorthosite pluton and spatially related Tessiarsuyungoakh intrusion, and metamorphic petrology of the adjacent Tasiuyak paragneiss, northern Labrador. Unpublished M.Sc. thesis, Memorial University of Newfoundland, St. John's, Newfoundland and Labrador, 219 pages.
- Thomas, A. and Morrison, R.S.
1991: Geological map of the central part of the Ugjoktok River (NTS 13N/5 and parts of 13M/8, and 13N/6), Labrador (with accompanying notes).
Government of Newfoundland and Labrador, Department of Mines and Energy, Geological Survey Branch, Map 91-160.
- Wasteneys, H., Wardle, R., Krogh, T. and Ermanovics, I.
1996: U-Pb geochronological constraints on the deposition of the Ingrid Group and implications for the Saglek-Hopedale and Nain craton – Torngat orogeny boundaries. *In* Eastern Canadian Shield Onshore-Offshore Transect (ECSOOT). Compiled by R.J. Wardle and J. Hall. The University of British Columbia, Lithoprobe Secretariat, Report 57, pages 212-228.
- Winchester, J.A. and Floyd, P.A.
1976: Geochemical magma type discrimination: application to altered and metamorphosed basic igneous rocks. *Earth and Planetary Science Letters*, Volume 28, pages 459-469. [https://doi.org/10.1016/0012-821X\(76\)90207-7](https://doi.org/10.1016/0012-821X(76)90207-7).
- Wood, D.A., Joron, J.L. and Treuil, M.
1979: A re-appraisal of the use of trace elements to classify and discriminate between magma series erupted in different tectonic settings. *Earth and Planetary Science Letters*, Volume 50, pages 326-336.